AFIT/GAE/ENY/96-J-3

Effect of Transient Body Force on the Performance of an Axial Grooved Heat Pipe

THESIS

Wen-Lung Wang
Maj, Republic of China

AFIT/GAE/ENY/96-J-3

Approved for public release; distribution unlimited

DISCLAIMER NOTICE

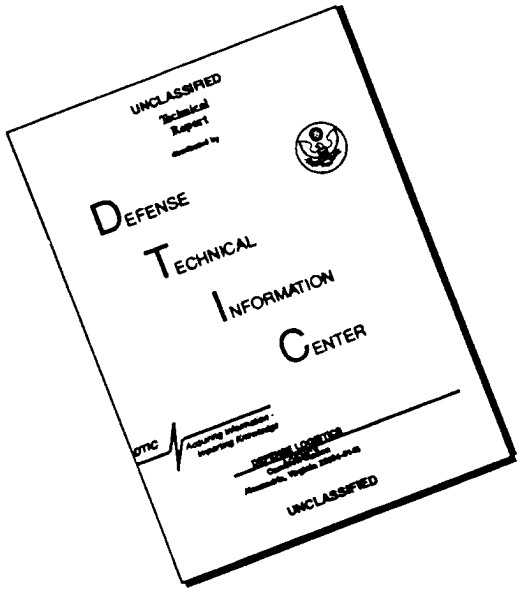

THIS DOCUMENT IS BEST QUALITY AVAILABLE. THE COPY FURNISHED TO DTIC CONTAINED A SIGNIFICANT NUMBER OF PAGES WHICH DO NOT REPRODUCE LEGIBLY.

The views expressed in this thesis are those of the author and do not reflect the official policy or position of the Department of Defense or the U. S. Government.

AFIT/GAE/ENY/96-J-3

Effect of Transient Body Force on the Performance of an Axial Grooved Heat Pipe

THESIS

Presented to the Faculty of the Graduate School of Engineering
of the Air Force Institute of Technology
Air University
In Partial Fulfillment of the
Requirements for the Degree of
Master of Science (Aeronautical Engineering)

Wen-Lung Wang, B.S.
Maj, Republic of China

June, 1996

Preface

It took quite a long time to make this thesis. Without the help and encouragement of several individuals, it could have never been done. The first of these is Lt. Colonel Jerry Bowman who has patiently and continuously guided me to focus and head in the right direction. I'll never forget his sense of humor. My thanks also goes to my course adviser, Dr. King. Without his guidance and help, I couldn't have found a thesis topic suitable for me to do. A special thanks goes to Jay Anderson and Andy Pitts, two laboratory experts, without whom most AFIT students would never graduate. Finally, my deepest thanks would go to my wife, Hui-Yueh, my daughter, Tina, and my son, William. Their patience, understanding and support helped me overcome all the obstacles during the whole AFIT years.

Wen-Lung Wang

Table of Contents

		Page
Preface		ii
List of Figures		v
List of Tables		vi
Abstract		x
I.	Introduction	1-1
	1.1 Thesis Statement	1-1
	1.2 History	1-1
	1.3 Background	1-1
	1.4 Purpose and Scope	1-4
II.	Theoretical Investigations	2-1
	2.1 Heat Pipe Geometry	2-1
	2.2 Heat Transport Limits	2-2
	2.3 The Pressure Balance Within a Heat Pipe	2-3
	2.4 Capillary Pressure in Axial Groove Wicks	2-6
	2.5 The Capillary Limit	2-7
III.	Experimental Investigation	3-1
	3.1 Experimental Equipment	3-1
	3.2 Calibration	3-2
	3.3 Heat Transfer Analysis	3-4
	3.4 Experimental Process	3-6
	3.5 Uncertainty Analysis	3-8
	3.6 Experimental Procedures	3-10

Page

IV. Experimental Results and Analysis 4-1

4.1 Extent of dryout in axial groove heat pipe 4-1

4.2 Time required for axial groove to dry out under different inclination angle 4-2

4.3 Time required for axial groove to rewet under different inclination angles and different tested duration 4-3

4.4 Time required for the heat pipe to return to its initial condition 4-4

V. Conclusions and Recommendations 5-1

5.1 Review for the whole experiment 5-1

5.2 Conclusions 5-1

5.3 Recommendations 5-2

Appendix A. Experimental Equipmint A-1

A.1 Coolant System A-2

A.2 Data Acquisition System A-2

A.3 Support System A-3

Bibliography BIB-1

Vita VITA-1

List of Figures

Figure		Page
1.1.	Components and Operation of a Conventional Heat Pipe	1-2
2.1.	Heat Pipe Cross-Sectional Drawing	2-1
2.2.	Heat Pipe Profile View	2-2
2.3.	The Theoretical Capillary Limit of The Tested Heat Pipe	2-3
2.4.	Circulation of Working Fluid Within a Heat Pipe	2-4
2.5.	Meniscus Geometry at the Liquid-Vapor Interface	2-7
3.1.	Heat Pipe Profile Thermocouple Location	3-2
3.2.	Calibration for Flow Meter	3-3
3.3.	Heat Transfer Profile of the Heat Pipe	3-4
3.4.	The Figure of Sample Experimental Data	3-8
4.1.	Temperature of TC Varies With Time Under Different Final Angle	4-5
4.1.	Temperature of TC Varies With Time Under Different Final Angle	4-6
4.1.	Temperature of TC Varies With Time Under Different Final Angle	4-7
4.2.	Dryout Length vs. Inclination Angle Comparison of Theoretical and Experimental Data	4-8
4.3.	Time for TC1 to Dry Out vs. the Final Inclination Angle	4-9
4.4.	Time for TC1 to Rewet vs. Test Duration	4-10
4.4.	Time for TC1 to Rewet vs. Test Duration	4-11
4.5.	Time for TC1 to Return to the Initial Condition vs. Test Duration	4-12
4.5.	Time for TC1 to Return to the Initial Condition vs. Test Duration	4-13
A.1.	The arrangement of the experimental equipment	A-1

List of Tables

Table		Page
2.1.	Heat Pipe Cross-Sectional Parameters	2-2
4.1.	The Theoretical Dryout Length vs. Inclination Angle	4-2

List of Symbols

Symble	Definition
A_c	area of the condenser (m^2)
A_e	area of the evaporator (m^2)
A_v	vapor flow area (m^2)
A_w	wick cross-sectional area (m^2)
c_p	the specific heat of the coolant $(J/kg\text{-}K)$
$c_{p,eg}$	the specific heat of the ethylen glycol $(J/kg\text{-}K)$
$c_{p,w}$	the specific heat of the water $(J/kg\text{-}K)$
DAS	data acquisition system
D_v	dynamic pressure coefficient $(N/m^2\text{-}W^2)$
F_l	liquid frictional coefficient $((N/m^2)/W\text{-}m)$
F_v	vapor frictional coefficient $((N/m^2)/W\text{-}m)$
g	gravitational force constant $(9.8\ m/sec^2)$
h_c	the convection heat coefficient of the condenser $(W/m^2\text{-}K)$
h_e	the convection heat coefficient of the evaporator $(W/m^2\text{-}K)$
K	wick permeability (m^2)
L_a	length of adiabatic section (m)
L_c	length of condenser section (m)
L_{do}	dried out length (m)
L_e	length of evaporator section (m)
$L_{e,do}$	evaporator effective length after dryout (m)
L_t	total length of the heat pipe (m)
$L_{t,do}$	total effective length after dryout (m)
$\dot{m}$	the mass flow rate (kg/sec)
n	number of grooves
P_c	capillary pressure (N/m^2)

P_{cm}	maximum capillary pressure (N/m^2)
$P_{cm,e}$	maximum effective capillary pressure (N/m^2)
P_l	liquid pressure (N/m^2)
P_v	vapor pressure (N/m^2)
Q	heat transfer rate (W)
Q_1	heat transfer rate between atmosphere and the evaporator (W)
Q_2	heat transfer rate between heat pipe wall and coolant (W)
Q_3	heat transfer rate into coolant (W)
Q_{cm}	capillary heat transfer limit (W)
$(QL)_{cm}$	capillary limit on heat transfer factor $(W\text{-}m)$
R_1	radius of curvature of the meniscus (m)
R_2	radius of curvature of the meniscus (m)
Re_v	Reynolds number of vapor
r_c	effective capillary radius (m)
$r_{h,v}$	vapor hydraulic radius (m)
T_{co}	coolant temperature (K)
T_{in}	coolant inlet temperature (K)
T_{out}	coolant outlet temperature (K)
T_r	room temperature (K)
$T_{w,c}$	wall temperature of the condenser (K)
$T_{w,e}$	wall temperature of the evaporator (K)
TC	thermocouple
TC_1	first thermocouple in evaporator section
TC_2	second thermocouple in evaporator section
TC_3	third thermocouple in evaporator section
TC_4	forth thermocouple in evaporator section
TC_5	fifth thermocouple in evaporator section
TC_6	sixth thermocouple in evaporator section

TC_7	seventh thermocouple in evaporator section
TC_8	eighth thermocouple in evaporator section
TC_9	coolant manifold inlet
TC_{10}	coolant manifold outlet
t_l	groove land thickness (bottom) (m)
W	groove opening (top) (m)
W_b	groove opening (bottom) (m)
Δc_p	the error in measuring c_p $(J/kg\text{-}K)$
$\Delta \dot{m}$	the error in measuring $\dot{m}$ (J/sec)
$\Delta P_\perp$	hydrostatic pressure $\perp$ to heat pipe axis (N/m^2)
ΔP_l	liquid pressure (N/m^2)
ΔP_v	vapor pressure (N/m^2)
ΔQ	the error in measuring Q (W)
ΔT	temperature difference (K)
$\Delta(\Delta T)$	the error in measuring ΔT (K)
x	axial position (m)
x_{ref}	reference axial position from which x is measured (m)
x_{min}	axial position where capillary pressure is minimum (m)
α	heat pipe groove angle (degree)
δ	groove depth (m)
λ	latent heat of vaporization (J/kg)
σ	surface tension coefficient (N/m)
ρ_{eg}	density of ethylen glycol (kg/m^3)
ρ_l	liquid density (kg/m^3)
ρ_v	vapor density (kg/m^3)
ρ_w	density of water (kg/m^3)
μ_l	liquid viscosity $(kg/m\text{-}sec)$
μ_v	vapor viscosity $(kg/m\text{-}sec)$
ψ	heat pipe inclination angle (radians)

Abstract

An experimental investigation was performed to determine the effect of transient body forces on the performance of an ammonia/aluminum axial groove heat pipe. The effects of increased body forces on the dryout and rewet performance were simulated by tilting the heat pipe to different inclination angles. Theoretical calculations predicted the dryout length varied with different final inclination angles. The steady state experimental work was performed by tilting the heat pipe from 0 degrees to different final inclination angles for a long period of time until totally dryout occurred. Then, from the plot of the changing temperature at each location along the heat pipe, the dryout length could be predicted. Under steady state condition, the percent error between the experimental and theoretical data differed by as low as 50 %. The transient experimental work was performed by tilting the heat pipe from different initial inclination angles to different final inclination angles under three duration conditions. The time for the heat pipe to dryout, rewet, and return to the initial condition was observed as a function of the initial inclination angles, the final inclination angles, and duration of the heat pipe at the final angle. The results revealed that the larger body force (or the larger final inclination angle) increased the dryout length, and increased the time to return to its initial condition. The duration of the adverse angle had less of an effect on the time to rewet. But the initial inclination angle has a strong effect on the time to rewet. When the initial inclination angle was 0 degrees, it took around 3 to 6 seconds to rewet. When the initial inclination angle became 1 degrees, it took around 8 to 12 seconds to rewet. When the initial inclination angle was 1.25 degrees, it took around 15 to 17 seconds to rewet.

Effect of Transient Body Force on the Performance of an Axial Grooved Heat Pipe

I. Introduction

1.1 Thesis Statement

Body forces will influence the liquid in a heat pipe wick. Wick dryout will be quicker for larger adverse body forces and longer duration body forces will result in longer times for rewet.

1.2 History

The principle of the heat pipe was conceived in 1944 by Gaugler. However, it was not widely publicized until 1964 when Grover and his colleagues at the Los Alamos Scientific Laboratory independently reinvented the concept, named it the heat pipe, and developed its application ([2]). Over the past three decades, the heat pipe has been developed into a highly effective and reliable heat transmission device. For examples, it has been used in such diverse applications as nuclear reactor cooling, road/runway/bridge de-icing, electronic component cooling, aircraft leading edge cooling, and spacecraft thermal control ([3],[2]).

1.3 Background

Though, nowadays, heat pipes have been widely used, and lots of papers have been written, more can be learned. Hence, a brief discussion of heat pipe operating principles will be useful as background for this thesis.

The conventional form of the heat pipe is a closed tube or chamber of different shapes whose inner surfaces are lined with a porous capillary wick. The wick is

saturated with the liquid phase of a working fluid and the remaining space contains the vapor phase ([2]).

In operation, as shown in Fig. 1.1, heat is applied to one end of the heat pipe,

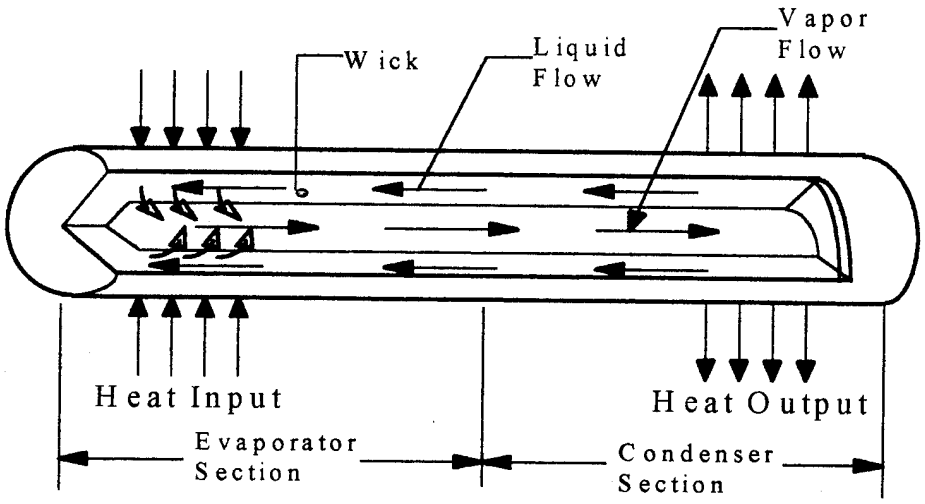

Figure 1.1 Components and Operation of a Conventional Heat Pipe

called the evaporator section, and removed from the other end of the heat pipe, the condenser section. Within the evaporator section, heat applied by an external source causes liquid to evaporate from the wick, resulting in a pressure difference which drives the vapor to the condenser section. This vapor then condenses on the cooler surface of the condenser, releasing the latent heat of vaporization to a heat sink. Depletion of liquid by evaporation causes the liquid-vapor interface in the evaporator to enter into the wick surface where a capillary pressure is developed. This capillary pressure pumps the condensed liquid through the wick back to the evaporator for re-evaporation. So, the heat pipe can continuously transfer the latent heat of vaporization from the evaporator section to the condenser section.

Under certain conditions, there are some heat transport limits within the heat pipe. The capillary limit is reached when the maximum capillary pressure is lower than the sum of the liquid and vapor pressures drops within the wick. The sonic

occurs when vapor leaves the evaporator at sonic speed and the flow becomes choked. The entrainment limit occurs when the flow actually tears liquid from the surface of the liquid-vapor interfaces and decreases the amount of working fluid which reaches the evaporator. And lastly, the boiling limit is reached when heat flux, added to the evaporator and flowing through the wall and wick, exceeds a certain critical value, causing the liquid in the wick to boil. Among these limits, the capillary limit is most important to this research. When the capillary limit is exceeded, the wick of the heat pipe dries out, (appropriately termed 'dryout'), and the working fluid can no longer be pumped to the evaporator section, halting the heat transfer cycle.

As a result of its capability of transporting heat over a long distance without any need for external power to circulate the heat transfer fluid, the heat pipe has been widely used in both fields of spacecraft and aircraft. Of more significance to the Air Force is the proposed use of heat pipes to reduce peak temperature and large thermal gradients at leading edges of the wing and engine nacelles of hypersonic aircraft such as the National Aerospace Plane.

Now the heat pipe has been widely used, and several papers relating to the effect of body forces on heat pipe performance have been found which are useful in understanding previous research in this area ([5], [6], [7], [8], [9], [10], [11], [12]). The bulk of knowledge on body force effects can be divided into that dealing with steady-state body forces (constant accelerations or vibrations) and that dealing with transient body force. To date, based on the experimental work reference, there is sufficient evidence to show that body forces do influence the liquid flow in a capillary structure. These body forces act on the liquid and move it in a manner that can cause a dryout condition. These same body forces can effect a rewet of the dried-out region as well.

1.4 Purpose and Scope

The purpose of the current experimental study was to provide a reference regarding the effects of dryout and rewet on heat pipe performance. Included in this study was an investigation of the effects of dryout length and rewetting time under different inclination angles (including steady-state and transient conditions) on an ammonia/axial groove wick heat pipe, simulating this heat pipe being used in an accelerating aerospace vehicle. To accomplish this, the heat pipe was set at initial angles of 0, 1 and 1.25 degree, and final angles of 1.75, 2, 3, and 4 degree. For the sake of getting a higher heat transfer rate on the heat pipe, a fan, always set at high speed position, was used during the whole experiment. The results of steady-state experiments will be used to compare the heat pipe performance with the theoretical results which were run by the computer code written in FORTRAN 77. This research was the first to actually evaluate the effects of dryout and rewet in an axial groove wick heat pipe in a transient body force environment.

II. Theoretical Investigations

In this chapter, the performance of the tested heat pipe will be briefly discussed. Most of the pages will be used to discuss the theory of the capillary limit and to determine some useful equations. These equations will be used to get theoretical data for use in later comparison.

2.1 Heat Pipe Geometry

The heat pipe used for this experiment was supplied by Dynatherm Corporation. It was an axial-groove wick heat pipe of extruded aluminum and was filled with 8.6 grams of anhydrous ammonia as a working fluid. Fig. 2.1 shows the tested heat pipe in cross section while Table 2.1 points out critical heat pipe dimensions. The profile of the tested heat pipe is shown in Fig. 2.2, including the dimensions for evaporator and condenser section.

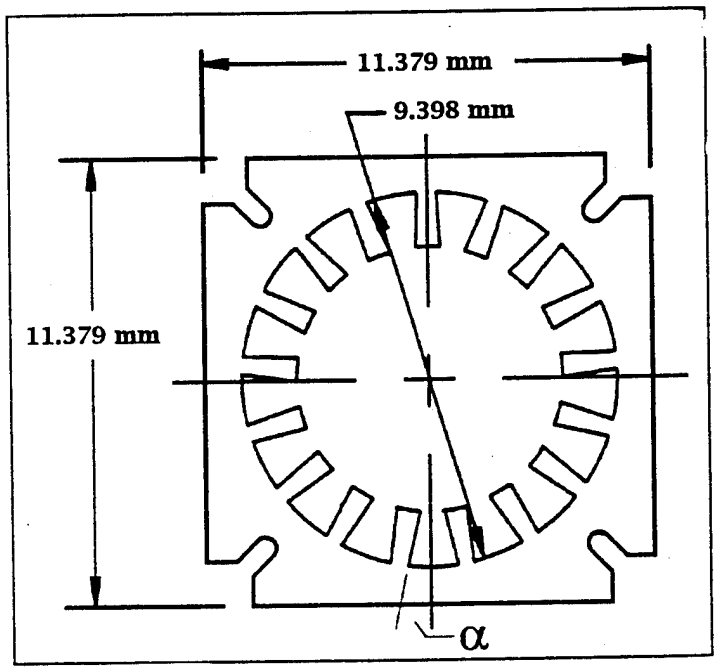

Figure 2.1 Heat Pipe Cross-Sectional Drawing

Table 2.1 Heat Pipe Cross-Sectional Parameters

Land Thickness (Bottom)	t_l	**0.020 in**	**0.508 mm**
Groove Opening (Top)	**W**	**0.025 in**	**0.635 mm**
Groove Opening (Bottom)	W_b	**0.048 in**	**1.219 mm**
Groove Depth	δ	**0.055 in**	**1.397 mm**
Groove Angle	α	**13.9^0**	**0.2426 rad**
Number of Grooves	**n**	**17**	**17**

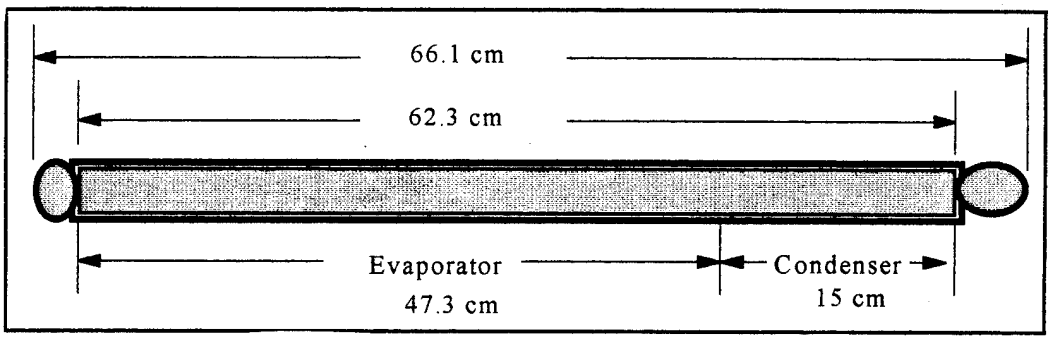

Figure 2.2 Heat Pipe Profile View

2.2 Heat Transport Limits

The operation of heat pipes is constrained by four operating heat transport limits. They are the sonic limit, the entrainment limit, the capillary limit and the boiling limit. The heat transport limits are functions of the heat pipe geometry, the working fluid properties, and the heat pipe operational environment. The last category includes heat pipe inclinations, heat pipe section lengths, and other external influences.

For this thesis, the capillary limit was most the important due to the influence of gravity on the liquid in the wick. The complete explanation and derivation for the capillary limit will be given later. Fig. 2.3 is a plot of the theoretical capillary limit of the tested heat pipe.

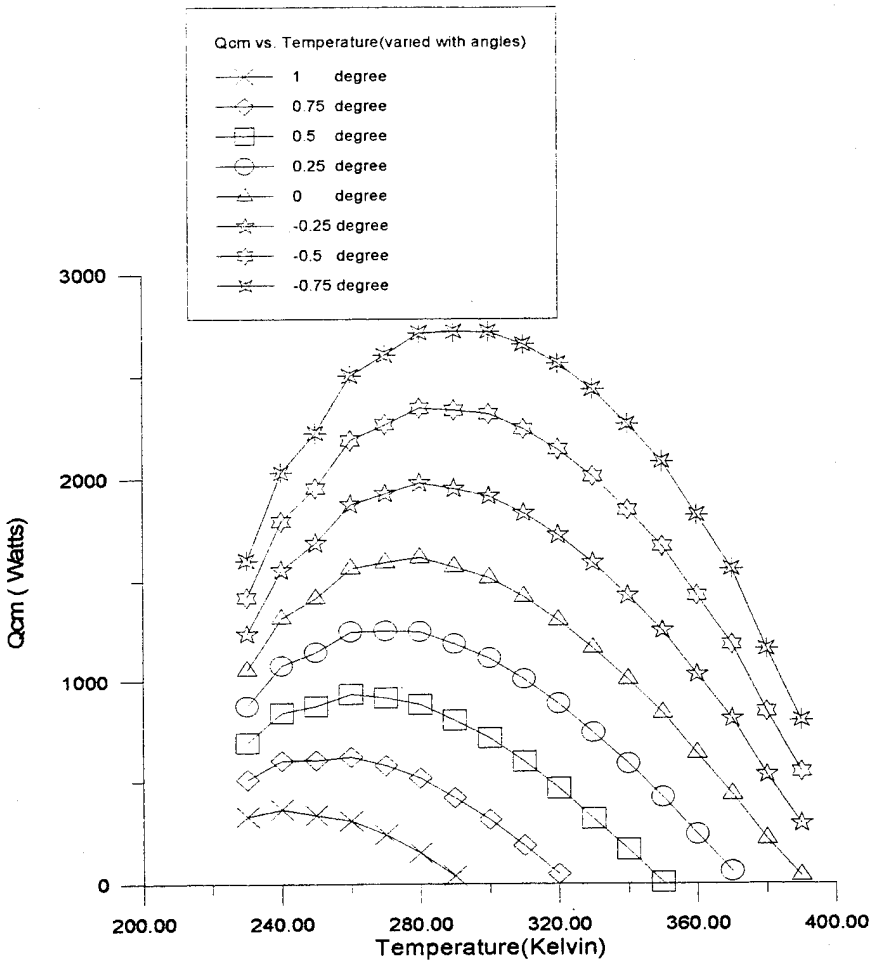

Figure 2.3 The Theoretical Capillary Limit of The Tested Heat Pipe

An examination of Fig. 2.3 reveals that the steeper the tilted angle, the smaller the capillary limit, Q_{cm}(it is defined as the heat transfer rate, Q, reaches a critical value as soon as the heat pipe begins to dryout.). This means that larger adverse body forces cause the wick to dryout at lower power levels.

2.3 The Pressure Balance Within a Heat Pipe

Though a heat pipe is mechanically simple, its inner functions are quite complex. Basically, the heat pipe depends upon a pressure balance to maintain its heat transport cycle. This section will briefly cover the basic heat pipe pressure balance. More details can be found in references ([2]) and ([4]).

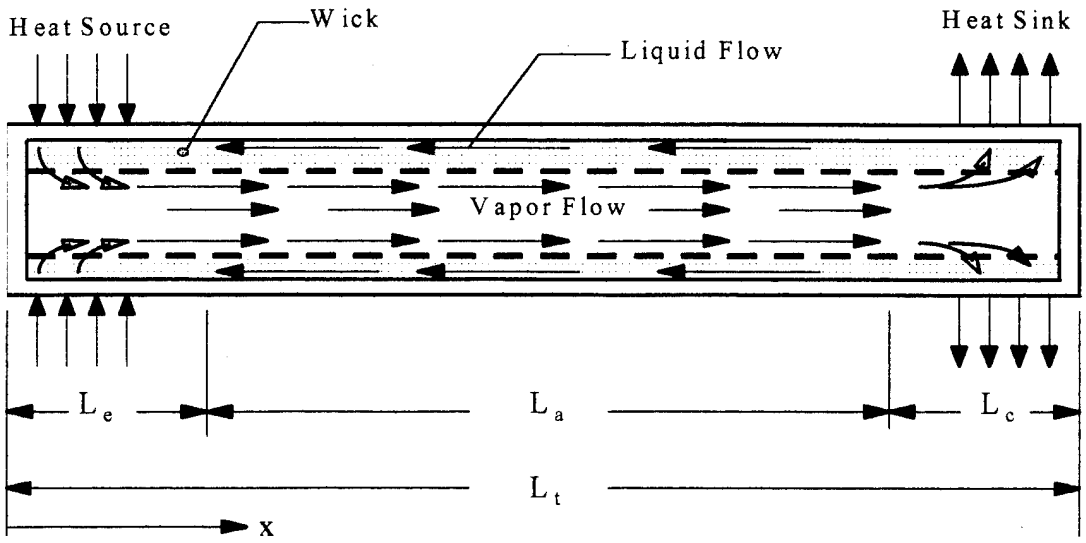

Figure 2.4 Circulation of Working Fluid Within a Heat Pipe

During steady state operation of a heat pipe as shown in Fig. 2.4, the working fluid in the vapor phase flows continuously from the evaporator section to the condenser, and it returns to the evaporator in the liquid phase. There exists a vapor pressure gradient along the vapor flow passage when the vapor flows from the evaporator to the condenser. There also exists a liquid pressure gradient as the condensed liquid flows back from the condenser to the evaporator ([2]: 33). Since the heat pipe is a sealed system, these two pressures must be balanced. This balance requires that along the length of the heat pipe the pressure at the liquid side of the liquid-vapor interface must be different from the pressure at the vapor side of the interface, except in the condenser, where the pressure difference is minimum, and equals to zero ([2]: 33). This pressure difference at the liquid-vapor interface is set up by the meniscus that forms at the liquid-vapor interface. Since molecules in a liquid attract each other, the molecules at the liquid-vapor interface experience a

force inward, forcing the liquid to take up a concave shape having minimum area ([4] :20). Surface tension is defined as the work required per unit area to increase the surface area of a fluid. A direct effect of surface tension is that the pressure on a concave surface is less than that on a convex surface, resulting in a pressure difference, or capillary pressure, at the interface. The pressure balance inside of a heat pipe can be described ([2]) as

$$[P_v(x_{ref})-P_v(x)]+[P_v(x)-P_l(x)]+[P_l(x)-P_l(x_{ref})]+[P_l(x_{ref})-P_v(x_{ref})] = 0 \quad (2.1)$$

The previously mentioned capillary pressure, P_c, is defined as the vapor pressure, P_v, minus the liquid pressure, P_l, or mathematically ([2] :33), as

$$P_c(x) = P_c(x_{ref}) + \Delta P_v(x - x_{ref}) + \Delta P_l(x_{ref} - x) \quad (2.2)$$

where

$$\begin{aligned}
P_c(x) &= \text{capillary pressure at position } x \\
&= P_v(x) - P_l(x)(N/m^2) \\
P_c(x_{ref}) &= \text{capillary pressure at reference position } x_{ref} \\
&= P_v(x_{ref}) - P_l(x_{ref})(N/m^2) \\
\Delta P_v(x - x_{ref}) &= \text{vapor pressure drop between } x \text{ and } x_{ref} \\
&= P_v(x) - P_v(x_{ref})(N/m^2) \\
\Delta P_l(x_{ref} - x) &= \text{liquid pressure drop between } x_{ref} \text{ and } x \\
&= P_l(x_{ref}) - P_l(x)(N/m^2)
\end{aligned}$$

The reference position, x_{ref}, is usually chosen to be at x_{min}, where P_c is equal to zero, so Eq. (2.2) reduces to

$$P_c(x) = \Delta P_v(x - x_{min}) + \Delta P_l(x_{min} - x) \tag{2.3}$$

2.4 Capillary Pressure in Axial Groove Wicks

The capillary pressure can also be expressed in terms of the meniscus of the liquid-vapor interface within the wick just as it can be expressed in terms of the pressure balance within the heat pipe, a direct effect of the working fluid's surface tension and the molecular attraction between its molecules.

When a meniscus is developed at the liquid-vapor interface, the Laplace-Young Equation ([2]:34) can be used to calculate the capillary pressure, $(P_v - P_l)$, as

$$P_c(x) = \sigma(\frac{1}{R_1(x)} + \frac{1}{R_2(x)}) \tag{2.4}$$

where R_1 and R_2, as shown in Fig. 2.5, are the principal radii of curvature of the meniscus and σ is the surface tension of the liquid in N/m.

For an axial groove, we can determine the capillary radius in a straightforward manner. One of the radii of curvature,(corresponding to the lengthwise meniscus), is infinity, and the other, (spanning the width of the groove), is equal to half of the groove width, ranging from infinity to half of the groove width depending on the amount of fluid in the groove ([2]:36). So the maximum capillary pressure is

$$P_{cm} = \frac{2\sigma}{r_c} \tag{2.5}$$

where r_c is the effective capillary radius.

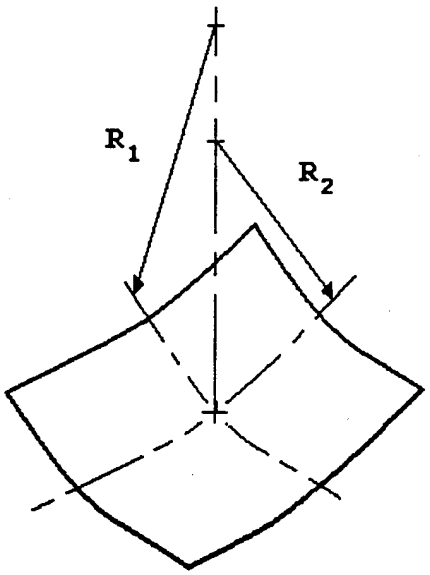

Figure 2.5 Meniscus Geometry at the Liquid-Vapor Interface

2.5 The Capillary Limit

The capillary limit occurs when liquid in the wick is evaporating more rapidly than capillary forces can replenish the liquid. This condition results in local wick dryout and increases wall temperatures ([1]:36). Hence,for continuing operation, the maximum capillary pressure, P_{cm}, must satisfy the relationship,

$$P_{cm} \geq \Delta P_l + \Delta P_v \tag{2.6}$$

where ΔP_l is the liquid pressure drop experienced by the working fluid in returning from the condenser to the evaporator and ΔP_v is the vapor pressure drop causing the vapor to flow from the evaporator to the condenser. If Eq. 2.6 is not satisfied,

then the wick will dryout in the evaporator section and the heat transport cycle will stop. At the maximum operating condition the capillary limit can be expressed by

$$P_{cm} = \Delta P_l + \Delta P_v \tag{2.7}$$

Referring back to Fig. 2.4, the liquid pressure drop in a wick can be obtained by integrating the liquid pressure gradient ([2]:38):

$$P_l(x_{min}) - P_l(x) = -\int_{x_{min}}^{x} \frac{dP_l}{dx} dx \tag{2.8}$$

For steady state, the liquid pressure gradient in the direction of liquid flow is related to the frictional drag and gravitational force by the equation ([2]:38):

$$\frac{dP_l}{dx} = -F_l Q \pm \rho_l g sin\psi \tag{2.9}$$

where Q is the local axial heat transfer rate in Watts, ψ is the angle of inclination of the heat pipe measured from the horizontal direction and F_l is the frictional coefficient for the liquid flow in $(N/m^2)/W\text{-}m$, defined as

$$F_l = \frac{\mu_l}{K A_w \lambda \rho_l} \tag{2.10}$$

Here, the variables in Eq. 2.10 are defined as follows :

$$\begin{aligned}
\mu_l &= \text{liquid viscosity } (kg/m - sec) \\
\rho_l &= \text{liquid density } (kg/m^3) \\
\lambda &= \text{latent heat of vaporization } (J/kg) \\
A_w &= \text{wick cross-sectional area } (m^2) \\
K &= \text{wick permeability } (m^2)
\end{aligned}$$

where K is a property of the wick structure and is tabulated for reference ([2]:42).

In Eq. 2.9, the $\pm$ sign is changed by g which is the gravitational acceleration. The gravitational force may be positive or negative depending on whether the liquid is flowing in a direction with or against g. In this thesis, an increase in acceleration forces was simulated by increasing the angle ψ.

Similarly, the vapor pressure drop in the heat pipe vapor flow passage can be calculated by integrating the vapor pressure gradient ([2]:43):

$$P_v(x) - P_l(x_{min}) = \int_{x_{min}}^{x} \frac{dP_v}{dx} dx \tag{2.11}$$

and also can be written in an alternative form:

$$\frac{dP_v}{dx} = -F_v Q - D_v \frac{dQ^2}{dx} \tag{2.12}$$

Here, F_v and D_v are, respectively, the frictional and dynamic pressure coefficients for the vapor flow. And F_v can be defined as follows:

$$F_v = \frac{(f_v Re_v)\mu_v}{2(r_{h,v})^2 A_v \rho_v \lambda} \tag{2.13}$$

where the variables in Eq. 2.13 are defined as follows :

$$\begin{aligned}
\mu_v &= \text{vapor viscosity } (kg/m - sec) \\
\rho_v &= \text{vapor density } (kg/m^2) \\
\lambda &= \text{latent heat of vaporization } (J/kg) \\
A_v &= \text{vapor flow area } (m^2) \\
f_v &= \text{vapor frictional coefficient}
\end{aligned}$$

Re_v = Reynolds number of vapor

$r_{h,v}$ = vapor hydraulic radius (m)

In section 2.3, the capillary pressure along the whole length of the heat pipe is required to solve Eq. 2.3, i.e.

$$P_c(x) = \Delta P_v(x - x_{min}) + \Delta P_l(x_{min} - x)$$

Substituting $\Delta P_v(x - x_{min})$ and $\Delta P_l(x_{min} - x)$ from Eqs. 2.8 and 2.11, into Eq. 2.3 results in

$$P_c(x) = \int_{x_{min}}^{x} (\frac{dP_v}{dx} - \frac{dP_l}{dx})dx \tag{2.14}$$

Of course, there exists a maximum possible capillary pressure for any liquid-wick combination, see Eq. 2.5. Besides, when a heat pipe is operating in a gravitational field and circumferential communication of liquid within the liquid is possible, then the maximum effective capillary pressure $P_{cm,e}$ available for axial transport of fluid will be decreased by the effect of the gravitational force in the direction perpendicular to the heat pipe axis ([2]:51), i.e.

$$P_{cm,e} = \frac{2\sigma}{r_c} - \Delta P_\perp \tag{2.15}$$

Combining Eq. 2.14 and 2.15 results in a general equation for the capillary limitation on heat load:

$$\frac{2\sigma}{r_c} - \Delta P_\perp = \int_{x_{min}}^{x} (\frac{dP_v}{dx} - \frac{dP_l}{dx})dx \tag{2.16}$$

For a conventional heat pipe, the minimum capillary pressure occurs at the end of the condenser, i.e. at $x = 0$, and the maximum capillary pressure occurs at the end of the evaporator, i.e. at $x = L_t$. Hence, Eq. 2.16 can be reduced to

$$\frac{2\sigma}{r_c} - \Delta P_\perp = \int_0^{L_t} (\frac{dP_v}{dx} - \frac{dP_l}{dx})dx \tag{2.17}$$

Substituting $\frac{dP_v}{dx}$ and $\frac{dP_l}{dx}$ from Eqs. 2.12 and 2.9, respectively, into Eq. 2.17 yields

$$\frac{2\sigma}{r_c} - \Delta P_\perp = \int_0^{L_t} (F_v Q - D_v \frac{dQ^2}{dx} + F_l Q + \rho_l g sin\psi)dx \tag{2.18}$$

In Eq. 2.18, since Q is equal to zero at both ends of the heat pipe, the second integration part at the right hand side yields zero. Hence, Eq. 2.18 can be written as

$$\frac{2\sigma}{r_c} - \Delta P_\perp - \rho_l g L_t sin\psi = \int_0^{L_t} (F_v + F_l)Q dx \tag{2.19}$$

In this thesis study, since the vapor flow is laminar and incompressible, the values of F_v and F_l are independent of heat transfer rates and they can be calculated, respectively, by Eqs. 2.10 and 2.13. Hence, the capillary limitation on the heat transport factor $(QL)_{cm}$ can be expressed as

$$\begin{aligned} (QL)_{cm} &= \int_0^{L_t} Q dx \\ &= \frac{(\frac{2\sigma}{r_c} - \Delta P_\perp - \rho_l g L_t sin\psi)}{F_l + F_v} \end{aligned} \tag{2.20}$$

For the case of uniform heat flux along both the evaporator and the condenser, the capillary limitation on the heat transport rate, Q_{cm} can be derived from the heat transport factor. That is

$$(QL)_{cm} = (0.5L_c + L_a + 0.5L_e)Q_{c,m} \tag{2.21}$$

where

$$
\begin{aligned}
L_e &= \text{length of the heat pipe's evaporator section } (m) \\
L_a &= \text{length of the heat pipe's adiabatic section } (m) \\
L_c &= \text{length of the heat pipe's condenser section } (m)
\end{aligned}
$$

In my experiment, there was no adiabatic section. So, $L_a = 0$ will be true throughout the whole study. Then, the capillary heat transport limit for this experiment yields

$$(Q)_{cm} = \frac{(QL)_{cm}}{0.50L_c + 0.5L_e} \tag{2.22}$$

Finally, we are going to talk about the dryout length. When an operating heat pipe is partially dried out, we know that the total heat pipe length and the length of the evaporator will change. They will be the functions of their original lengths minus the dryout lengths. They are

$$
\begin{aligned}
L_{t,do} &= L_t - L_{do} \\
&= 0.6234 - L_{do}
\end{aligned} \tag{2.23}
$$

and

$$
\begin{aligned}
L_{e,do} &= L_e - L_{do} \\
&= 0.4734 - L_{do}
\end{aligned} \tag{2.24}
$$

where L_{do} is a dried out length and $L_t = 0.6234$ m and $L_e = 0.4734$ m for the heat pipe studied during this research. Substituting Eqs. 2.23 and 2.24 into Eqs. 2.20 and 2.22, the dryout length can be expressed as

$$L_{do} = \frac{0.3117 - \frac{(\frac{2\sigma}{r_c} - 0.6234\rho_l g sin\psi)}{Q_{cm}(F_l + F_v)}}{0.5 + \frac{\rho_l g sin\psi}{Q_{cm}(F_l + F_v)}} \tag{2.25}$$

From Eq. 2.25, the whole picture of this thesis study has been vividly shown. The dryout length could be affected by the inclination angle, ψ, of the heat pipe and by the capillary limit, Q. In steady state condition, this equation will be used to calculate the theoretical dryout length which will be compared with the experimental data in Chapter 4.

III. Experimental Investigation

This chapter provides a brief overview of the experimental system and the instrument calibrations. The heat transfer analysis and its uncertainty is also discussed. Finally, the general experimental procedure is detailed.

3.1 Experimental Equipment

The equipment for this experiment consisted of three major subsystems, other than the heat pipe. The first subsystem is the coolant system which provides the heat sink to maintain the temperature of the condenser end of the heat pipe. In addition, by adjusting the coolant temperature and flow rate, the operating temperature of the heat pipe can be controlled. The data acquisition system (DAS) was used to record and display pertinent experimental data. Thermocouples (TCs) were used to measure temperature. These TCs mounted on the surface of the heat pipe were used to measured the surface temperature. These measured temperatures were acquired by another DAS and later saved. Fig. 3.1 shows the location and designation of the ten TCs used in this experiment. Finally, there is the structural subsystem. This system includes the iron frame, bolts and some styrofoam blocks. The iron frame was used to hold the heat pipe. One end of the frame was fixed and the other end was free to tilt up and down simulating this heat pipe experienced an acceleration. The bolts, including both fine and coarse threads, were used to tilt the heat pipe during steady state operating experiment. The styroform blocks made in different thickness were used to tilt the heat pipe during transient operating experiment. A detailed description and schematic of these three subsystems, along with their components, is provided in Appendix A.

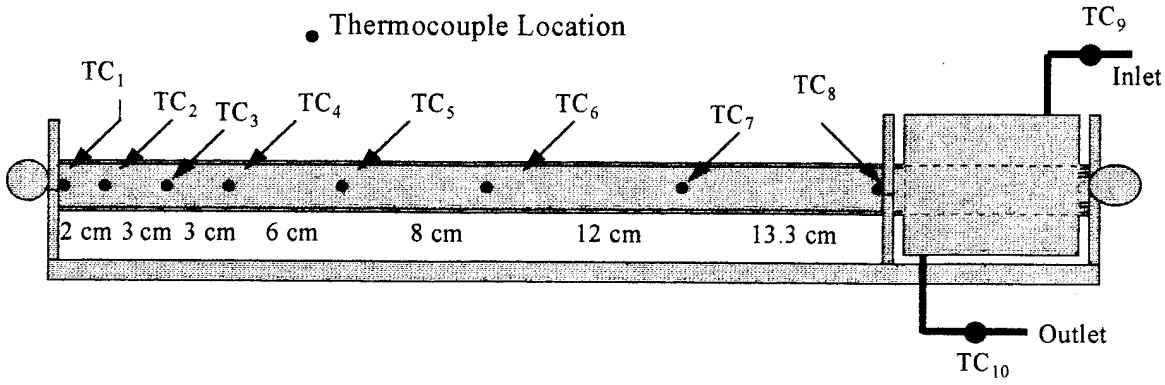

Figure 3.1 Heat Pipe Profile Thermocouple Location

3.2 Calibration

Accurate data is important to the thesis study. Before the experiment, we needed to quantify errors in the instruments used during the experimental process. I needed to calibrate the instrumentation, decreasing the uncertainty to a minimum. There are three devices used in the experiment that needed to be calibrated. They are the flow meter, the DAS, and an amplifier.

The flow meter, ranging from 0 to 150 ml/min, was used to read the flow rate of fluid which was pumping through the coolant system to remove heat from the condenser. First, the coolant system pump was turned on and the coolant temperature was set to -10, 0, and 10 degree C. The flow meter was set at the flow rate of 100 and 120 ml/min, individually. The coolant was diverted into a flask. The time was recorded for 100 ml to flow into the flask. Under different temperature and flow rate settings, the test was repeated five times and the average result for each setting was found. Fig. 3.2 shows the result of the flow rate calibration.

The DAS was used to acquire and record the data from each thermocouple (TC) mounted on the surface of the heat pipe for each experimental run. The epoxy used to attach the TCs onto the heat pipe adversely affected the heat conductivity

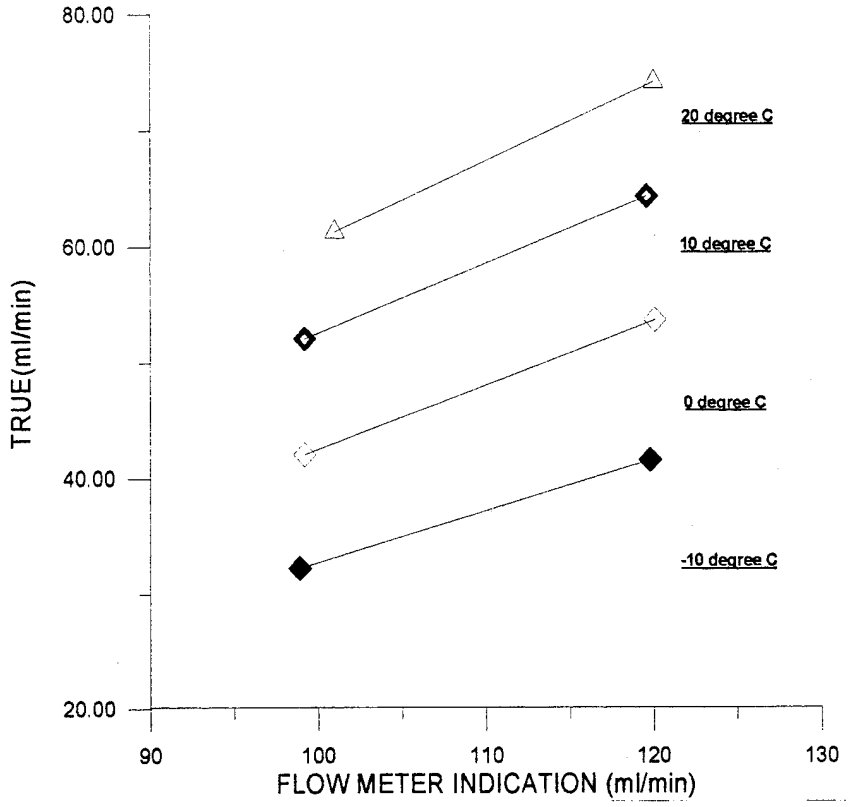

Figure 3.2 Calibration for Flow Meter

for each TC. It resulted in some readout errors among TCs. So, it was essential to develop a method to calibrate them. First, the coolant system was turned on with the heat pipe angle set at zero degree. Then, the coolant temperature was set at -15, 0, and 23 degree C for separate tests at different temperature and the flow meter was set at 120 ml/min. Once the steady state was reached, the DAS was used to acquire the data from all TCs. Since the heat pipe was not dried out under this condition, all the temperature readouts should be the same. Actually, there existed some differences among them. These differences were caused by the epoxy and the icepoints which were used with each TC. The average temperature for each setting temperature was found and defined as the standard value. A calibration equation was found for each TC which adjusted its readout to the standard value. It was used for data correction later.

When the experimental devices were first set up, some trial tests, using the DAS to acquire some data, showed that the noise in the TC signal was bigger than the TC output signal. An amplifier was used to enhance the signal before it was acquired by the DAS, and then the signal was divided by the amplifier when it was recorded by the PC. Since the amplifier would drift, it needed to be zeroed each day before the experiment.

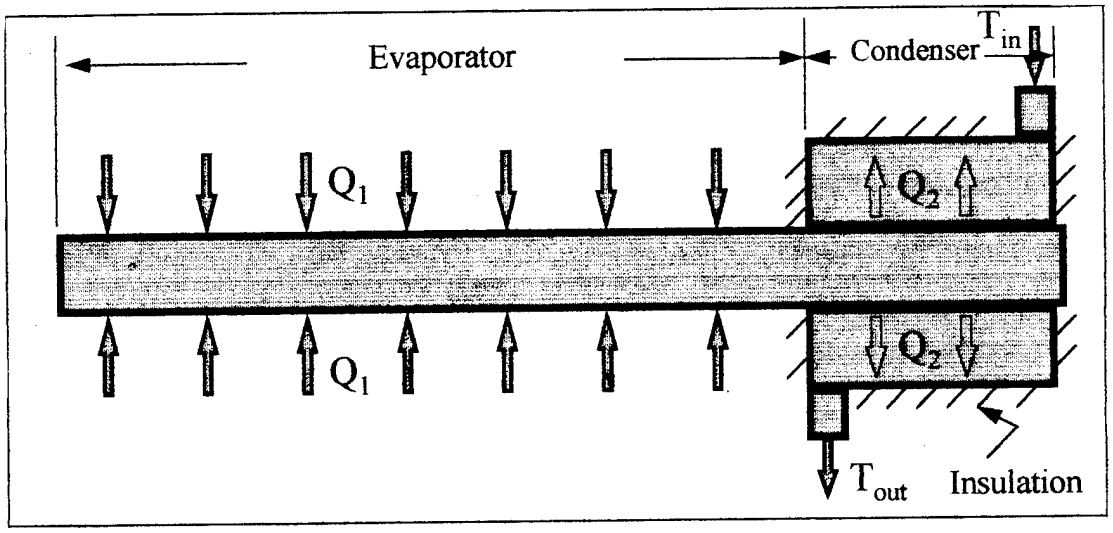

Figure 3.3 Heat Transfer Profile of the Heat Pipe

3.3 Heat Transfer Analysis

When the heat pipe is working, heat transfers occurred in and out of the heat pipe (see Fig. 3.3). The governing equations are as follows:

$$Q_1 = h_e A_e (T_r - T_{w,e}) \tag{3.1}$$

$$Q_2 = h_c A_c (T_{w,c} - T_{co}) \tag{3.2}$$

$$Q_3 = \dot{m} c_p (T_{out} - T_{in}) \tag{3.3}$$

where

$$T_{co} = \frac{T_{in} + T_{out}}{2}$$

The variables in the equations above are defined as follows:

h_e = the convection heat coefficient of the evaporator $(W/m^2 - K)$

h_c = the convection heat coefficient of the condenser $(W/m^2 - K)$

A_e = the area of the evaporator (m^2)

A_c = the area of the condenser (m^2)

T_r = the room temperature (K)

T_{co} = the coolant temperature (K)

$T_{w,c}$ = the wall temperature of the condenser (K)

$T_{w,e}$ = the wall temperature of the evaporator (K)

$\dot{m}$ = the mass flow rate (kg/sec)

c_p = the specific heat of the coolant $(J/kg - K)$

In Eq. 3.1 or Eq. 3.2, h_e and h_c were not known. Hence, Eq. 3.3 was used to find Q because $\dot{m}$, c_p , T_{out} , and T_{in} were easily measured. Note that the coolant used in this experiment was a mixture of 50 % water and 50 % ethylene glycol. Thus the

value of c_p was calculated by the equation as follows:

$$c_p = \frac{c_{p,w}\rho_w + c_{p,eg}\rho_{eg}}{\rho_w + \rho_{eg}} \tag{3.4}$$

The variables in the equation above are defined as follows:

$$\begin{aligned} c_p &= \text{the total specific heat } (J/kg - K) \\ c_{p,w} &= \text{the specific heat of water } (J/kg - K) \\ c_{p,eg} &= \text{the specific heat of ethylene glycol } (J/kg - K) \\ \rho_w &= \text{the density of water } (kg/m^3) \\ \rho_{eg} &= \text{the density of ethylene glycol } (kg/m^3) \end{aligned}$$

From the equations above, there are some key variables that can affect the value of Q. They are h, ΔT, and $\dot{m}$. If we need a higher Q which can cause the heat pipe to dryout easily, we had better make good use of these factors. In this experiment, h was enhanced by setting a high speed fan blowing directly to the heat pipe and $\dot{m}$ was increased by setting the flow meter at the 120 ml/min position. Note, here, that $\dot{m}$ and ΔT are related to each other. If we get a bigger $\dot{m}$, ΔT will become smaller, and vice versa. So, 120 ml/min is a proper value to get a maximum Q. Since the working fluid in the heat pipe, ammonia, has a high vapor pressure, it was not suitable to use a heater to heat the heat pipe. Hence, throughout this experiment, convection from the room temperature was used as a heat source. This turned out to limit to the heat transfer into the heat pipe.

3.4 Experimental Process

Before acquiring any convincing data for the thesis study, some parameters needed to be established and confirmed. First of all was to make sure the setup

was not affected by outside influences. For example, to ensure all the devices were well grounded, or some test section of the heat pipe, like condenser, has been well shielded yet. For the sake of getting a reliable heat transport, Q, in the heat pipe, the condenser section was wrapped with 3.5 cm radius styroform and layers of aluminum tape. Thus, any possibility of heat loss from condenser was minimized. Lastly, to make sure the inclinometer was working well. For the purpose of preventing it from showing error owing to running out of electricity, a new battery was replaced before the test. The digital inclinometer was used to measure the inclination of the heat pipe during the experiment. Its range of error is $\pm$ 0.05 degree for the inclination angle between 0–20 degree and $\pm$ 0.1 degree between 20–60 degree.

Once all the setup was checked, determining wick dryout needs to be defined. In Chapter 2, the heat pipe wick dryout was mentioned as a condition in which the working fluid is vaporized and cannot be replenished. It could be recognized as the wall temperature of evaporator increased rapidly near the room temperature. Especially, when the inclination angle got higher, the wall temperature of the evaporator would approach or equal the room temperature.

When experimental data has been collected and plotted, some important times were measured from each figure using Tecplot. In Fig. 3.4, the heat pipe was tilted from the initial inclination angle of 1 degree to the final inclination angle of 2 degree at time t_0, and the duration was 7 minutes. Then, the temperature of the heat pipe continuously increased to the point labeled t_2 where the slope became steeper. This was the time when the heat pipe dried out at the thermocouple location. Since the fluid in the wick has not been replenished until the heat pipe was tilted down, the temperature keeps rising, approaching room temperature. The heat pipe was tilted down at time t_1. The time t_3 was viewed as the total rewetting point. Since the heat pipe has been rewtted after time t_3, the temperature quickly decreases to the initial temperature. Time t_4 was viewed as the time when the heat pipe totally returned to the initial condition. Other than the times mentioned above, there are some other

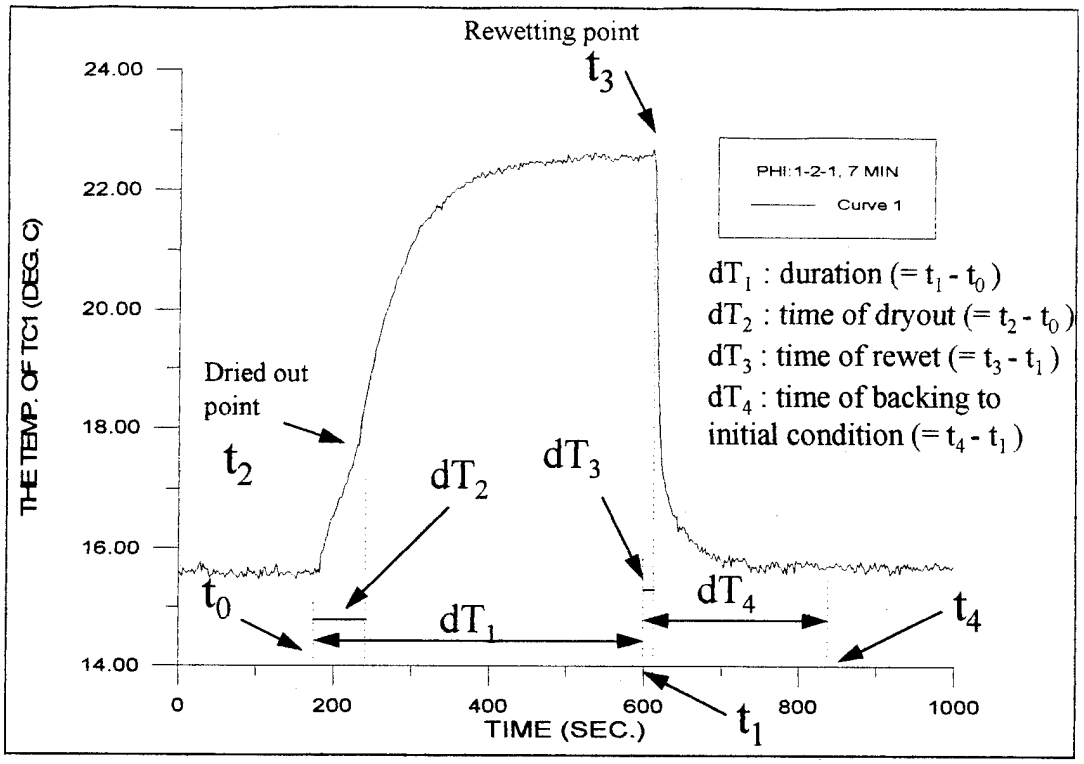

Figure 3.4 The Figure of Sample Experimental Data

times which need to be described. dT_1 was the tested duration, dT_2 was the time to dryout, dT_3 was the time to rewet, and dT_4 was the time to return to the initial condition. All of the times mentioned above will be used in Chapter 4.

3.5 Uncertainty Analysis

When considering the overall uncertainty in this experiment, Equation 3.3 which was related to the capillary limit was studied. This was because only these factors were used in the analysis of this research effort. For a total understanding of all sources of error in this thesis, they will be summarized in this section. Additionally, the overall experimental uncertainties for the capillary limit on the heat transport rate will be presented as well.

The error sources were: 1) an error of $\pm$ 0.2 degree in setting the heat pipe inclination, 2) a $\pm$ 2 second error in determining the duration for dryout and rewet, 3) a $\pm$ 0.01 m error in determining the length of the dried out region, 4) a $\pm$ 0.5 degree C error in reading each temperature, resulting in a $\pm$ 1 degree C error in determining temperature differences, or ΔT_s.

To determine the overall experimental uncertainty, the root–sum square method of determining error was used. Recall Eq. 3.3, shown as follows:

$$Q = \dot{m} c_p (T_{out} - T_{in})$$

So, using the root–sum square method, the Equation of the overall experimental uncertainty is described by

$$\Delta Q = [(\frac{\partial Q}{\partial \dot{m}} \Delta \dot{m})^2 + (\frac{\partial Q}{\partial c_p} \Delta c_p)^2 + (\frac{\partial Q}{\partial (\Delta T)} \Delta (\Delta T))^2]^{\frac{1}{2}} \tag{3.5}$$

where

$$\frac{\partial Q}{\partial \dot{m}} = C_p \Delta T \tag{3.6}$$

$$\frac{\partial Q}{\partial c_p} = \dot{m} \Delta T \tag{3.7}$$

$$\frac{\partial Q}{\partial (\Delta T)} = \dot{m} C_p \tag{3.8}$$

Substituting Eqs. 3.5, 3.6 and 3.7 into Eq. 3.4, yields

$$\frac{\Delta Q}{Q} = [(\frac{\Delta \dot{m}}{\dot{m}})^2 + (\frac{\Delta c_p}{c_p})^2 + (\frac{\Delta (\Delta T)}{\Delta T})^2]^{\frac{1}{2}} \tag{3.9}$$

The variables in Eq. 3.8 are defined as follows:

Q = the heat transfer rate (W)

ΔQ = the error in measuring Q (W)

$$
\begin{aligned}
\dot{m} &= \text{the mass flow rate } (kg/sec) \\
\Delta\dot{m} &= \text{the error in measuring } \dot{m} \ (kg/sec) \\
c_p &= \text{the specific heat } (J/kg-K) \\
\Delta c_p &= \text{the error in measuring } c_p \ (J/kg-K) \\
\Delta T &= \text{the temperature difference } (K) \\
\Delta(\Delta T) &= \text{the error in measuring } \Delta T \ (K)
\end{aligned}
$$

In this experiment, Q is around 15 W, $\dot{m} = 9.57 \times 10^{-4}$ kg/sec , $\Delta\dot{m} = 10^{-6}$ kg/sec, c_p = 3210 J/kg-K, Δc_p = 1 J/kg-K, ΔT = 6 K, $\Delta(\Delta T)$ = 1 K. Hence, ΔQ = 2.55 W, or about 17 %.

3.6 Experimental Procedures

In order to assure each of the experimental steps was performed in exactly the same way, a strict procedure was developed as follows:

Experimental Running Procedures

1. Zero the Amplifier
2. Set the fan at high speed position
3. Turn on the DAS and set up the acquiring data for trigger
4. Set coolant bath temperature and coolant flow rate
5. Set the heat pipe to the initial inclination angle
6. Allow the system to come to equilibrium
7. Tilt up the heat pipe to the wanted inclination angle and record the time
8. Leave the heat pipe tilted for the specified duration
9. Tilt the heat pipe down to the initial inclination angle

10. Wait until data acquisition is complete and see whether the data is proper or not (If yes, then save it. If not, then redo it again)
11. Allow the system to stabilize (15 to 20 minute).
12. Repeat steps 5 to 10 to get another set of data

IV. Experimental Results and Analysis

This chapter shows the results of the experiment conducted to achieve the objectives of this thesis. The objectives were to: 1) observe the extent of dryout in an axial groove wick heat pipe operating at different inclination angles and compare the results with theory, 2) observe the time for the heat pipe to dry out as a function of initial inclination angle, final angle and duration at the final angle, 3) observe the time for the heat pipe to rewet as a function of initial inclination angle, final angle and duration at the final angle, 4) observe the time for the heat pipe to return to its initial condition. In the beginning of each section, the experimental results will be described followed by an analysis of the data.

4.1 Extent of dryout in axial groove heat pipe

Under steady state conditions, when the axial groove heat pipe was tilted up from the horizontal position to some inclination angle, partial dryout was observed in the heat pipe. As shown in Fig. 4.1, the higher the final inclination angle, the longer the dryout length. Also, from Table 4.1, there is a vivid trend showing that the capillary limit, Q_{cm}, decreases as the final inclination angle increases. The capillary limit in Table 4.1 was calculated with Eq. 3.3 while the values of the variables used were $\dot{m} = 9.6 \times 10^{-4}$ kg/sec, $c_p = 3210$ J/kg-K, and ΔT was the difference between T_{in} and T_{out}. Note, here, that $\dot{m}$ and c_p were treated as constant and the uncertainty of them were lower than 0.3 %.

In Table 4.1, the theoretical values of L_{do} were calculated using Eq. 2.24. Here, the operating temperature of the heat pipe, T_l, was the average temperature of the coolant temperature, T_{co}, and the non-dryout average temperature along the heat pipe.

Fig. 4.2 shows that the gap between the theoretical data and the experimental values. The experimental values were measured from the plots shown in Fig. 4.1.

Table 4.1 The Theoretical Dryout Length vs. Inclination Angle

Inclination angle (degree)	Operating Temperature (K)	The Capillary Limit (W)	Dryout length (m)
0	284.7	16.46	0
1	284.9	15.32	0
1.25	285.3	14.79	0.097
1.50	286.7	14.85	0.189
1.75	286.9	14.26	0.251
2	286.9	13.13	0.297
3	285.7	10.35	0.404
4	286.6	10.54	0.459

It is very interesting to note that the percent error between them becomes smaller when the inclination angle gets bigger.

When the heat pipe is operating, as soon as the heat transfer rate, Q, exceeds the capillary limit, Q_{cm}, the heat pipe begins to dry out. For small inclination angles, the heat pipe required more Q to cause the dryout than at bigger inclination angle. So, if there was some energy loss from the devices, like the connectors or flow gauge, etc., this would cause the insufficiency of the Q to dry out the heat pipe. That could explain part of the error in the dryout length at the small inclination of the experimental part reaches 100 % (inclination angle was 1.25). In addition, the error might be caused by estimating the dry out length from the experimental data.

4.2 Time required for axial groove to dry out under different inclination angle

For the sake of easily understanding the time for the heat pipe to dry out, TC1 was chosen and observed during this and following sections. TC_1 was located at the end of the evaporator and was the first to indicate a raise in temperature due to dryout and the last thermocouple to return to steady state after rewet. For

the purpose of narrowing the error when the extent of dryout was measured from each plot, a useful software called Tecplot was used to zoom in on the plot to get an accurate observation. The uncertainty of the dryout temperature is under 0.2 degree C.

In Fig. 4.3, the upper line shows that the steeper the final inclination angle, the shorter the time to dryout. The middle line shows almost the same tendency as the upper one. The lower line shows that the time to dry out for the heat pipe with the highest final inclination angle is a slightly longer than other small inclination angle's. From the whole plot, it is interesting to note that for most of the data the higher the initial inclination angle, the less the time to dry out.

From Chapter 2, it has been mentioned that the steeper the inclination, the smaller the capillary limit, Q_{cm}. This trend can be seen in Fig. 4.3. For the upper two graphs, dryout occurred faster for higher angles. This indicates that less heat flux is required for dryout to occur.

4.3 Time required for axial groove to rewet under different inclination angles and different tested duration

In order to observe whether longer duration body forces will result in longer time for rewet, three intervals describing the time the heat pipe was exceeding the capillary limit were studied. They are 2, 4, and 7 minutes.

In Fig. 4.4(a), the time required for each heat pipe to rewet seems quite close independent of the duration of the dryout transient. In Fig. 4.4(b), there is a vivid trend showing that the bigger the final angle, the longer the rewetting time. Fig. 4.4(c) shows that the time required for the heat pipe to rewet is around 15 to 17 seconds for all final angles, other than the final angle at 1.75 degree.

The rewetting time is defined as the time period for the working fluid to refresh the wick. It is measured by using the time when the temperature starts to drop minus the time when the heat pipe was tilted down. In the theoretical point of view, longer

point of view, longer duration body forces should result in longer time for rewet. From the three plots, this is illustrated. An interesting point that needs to be mentioned here is that the initial angle has a strong affect on the rewetting time. The larger the initial angle the more difficult it will be for liquid to rewet the wick due to the larger adverse body force acting on the fluid in the wick. From Fig. 4.4(a), the rewetting time is shorter than the other two plots whose initial angles were not zero. When the initial angle exceeds 1.25 degree, like Fig. 4.4(c), the time for rewet increases. The duration of the adverse angle had less of an affect on the time to rewet.

4.4 Time required for the heat pipe to return to its initial condition

The slopes in Fig. 4.5(a), (b), (c) reveal that the longer the duration of dryout, the longer the time to return to the initial condition. As a whole, it takes only a few minutes (less than 6 minute) for the tested heat pipe to return to its normal condition.

During the experiment, since the temperature of all TCs fluctuated before and after the tested heat pipe was tilted up and down, it was hard to use a standard horizontal line to find the exact times when the heat pipe returned to its initial condition. Hence, the error was quite big, around $\pm$ 50 seconds. Here was an arguing point which was left to be re–examined by more accurate methods in the future.

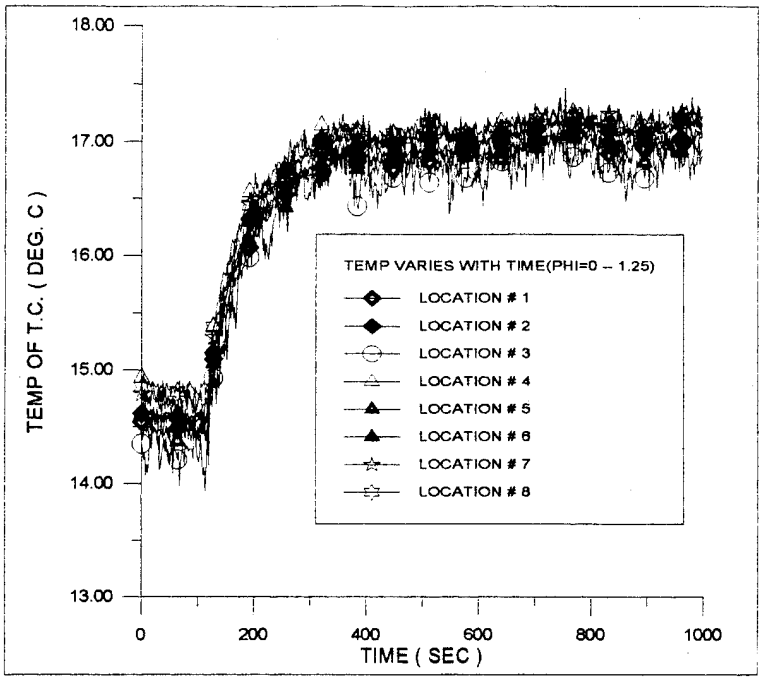

(a)

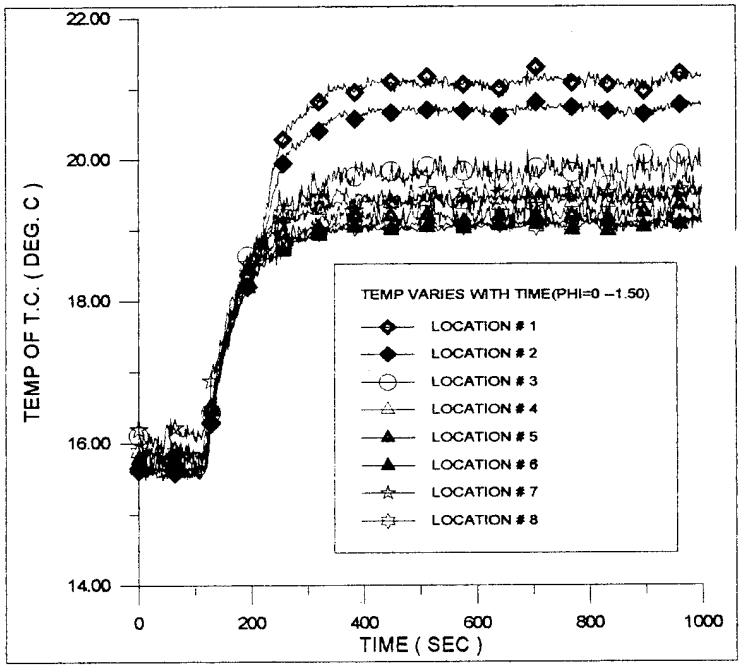

(b)

Figure 4.1(a),(b) Temperature of TC Varies With Time Under Different Final Angle

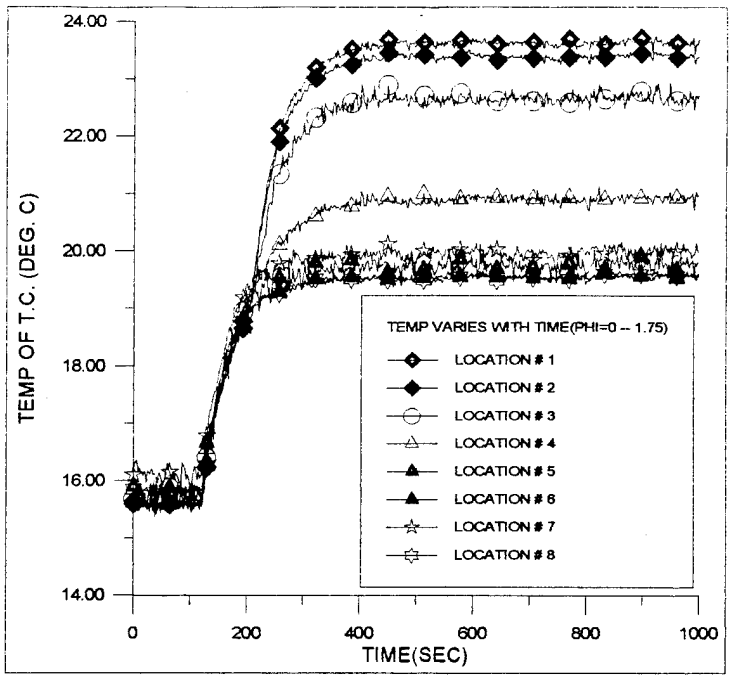

(c)

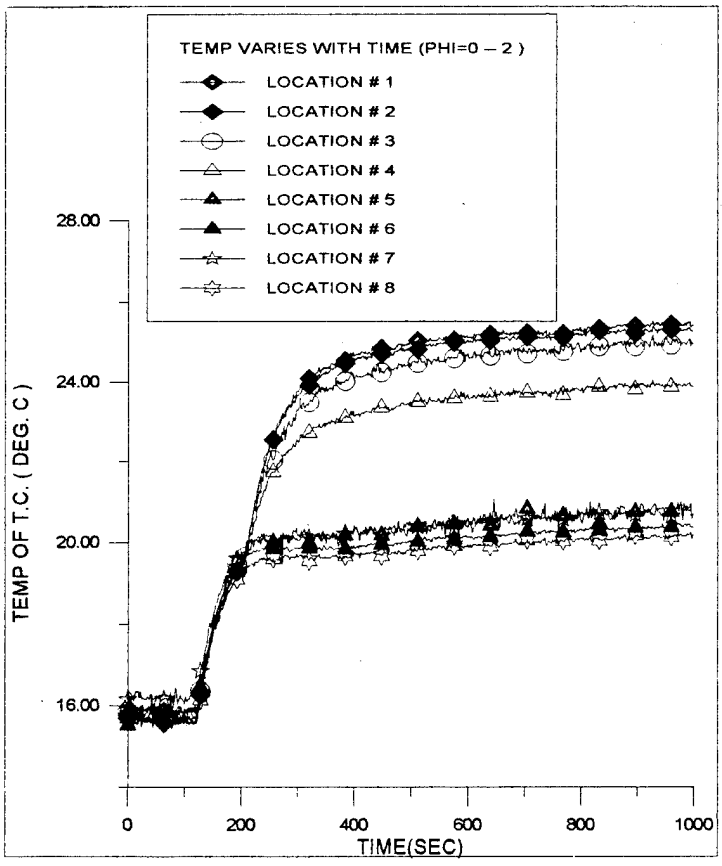

(d)

Figure 4.1(c),(d) Temperature of TC Varies With Time Under Different Final Angle

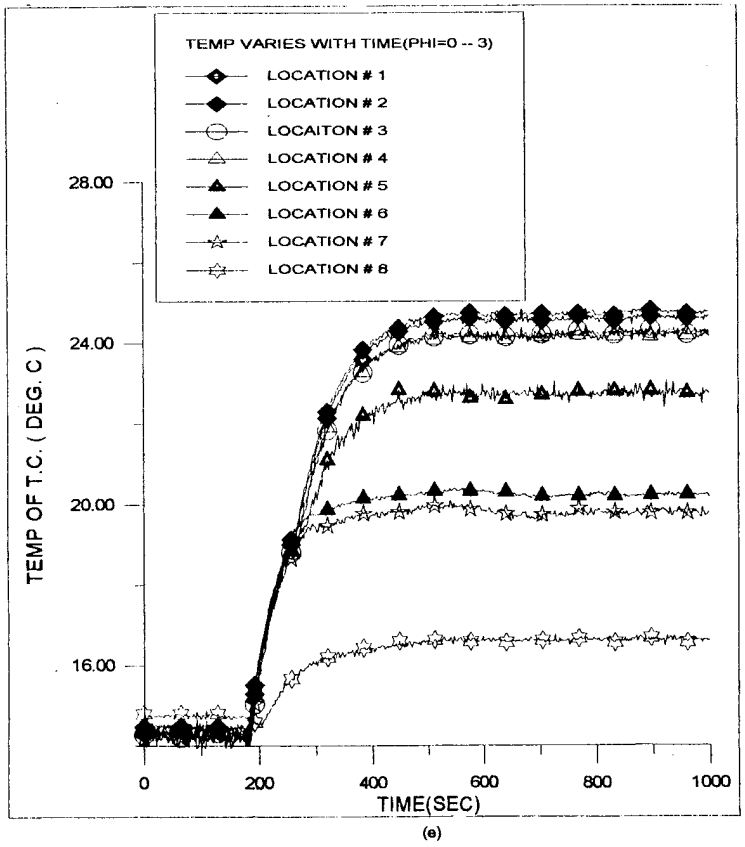

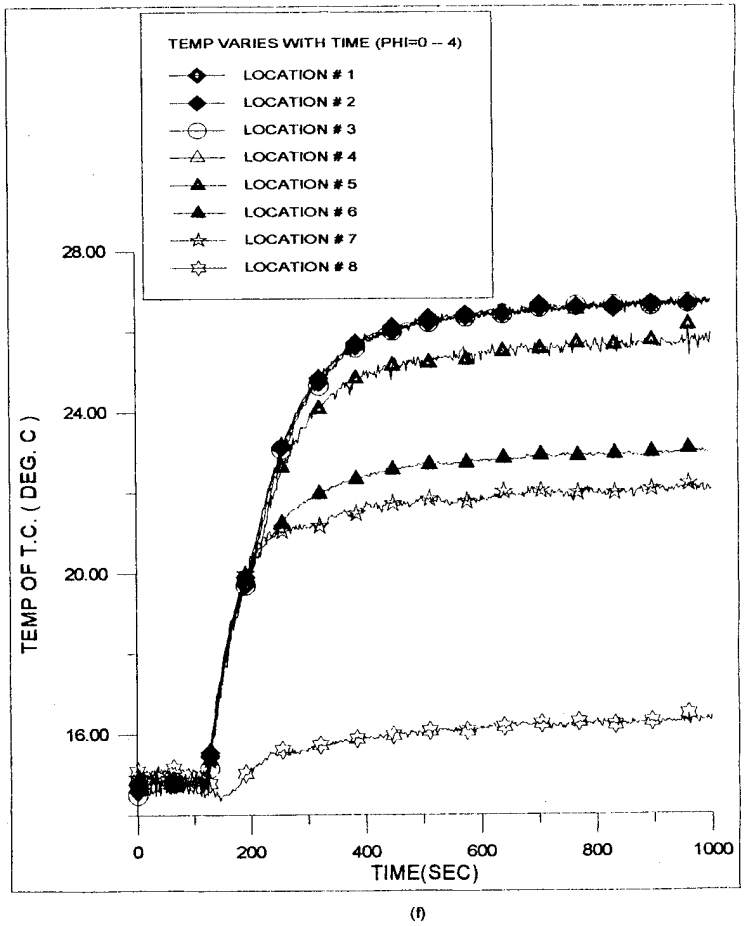

Figure 4.1(e), (f) Temperature of TC Varies With Time Under Different Final Angle

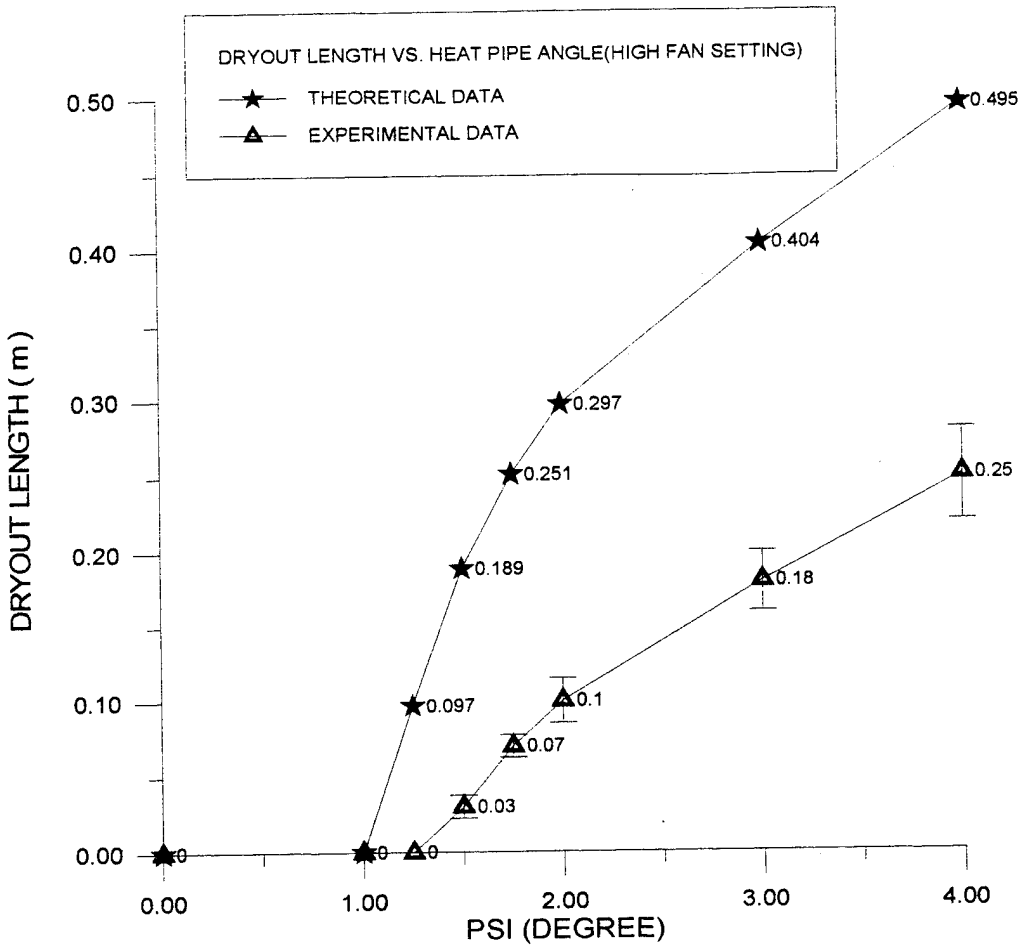

Figure 4.2 Dryout Length vs. Inclination Angle Comparison of Theoretical and Experimental Data

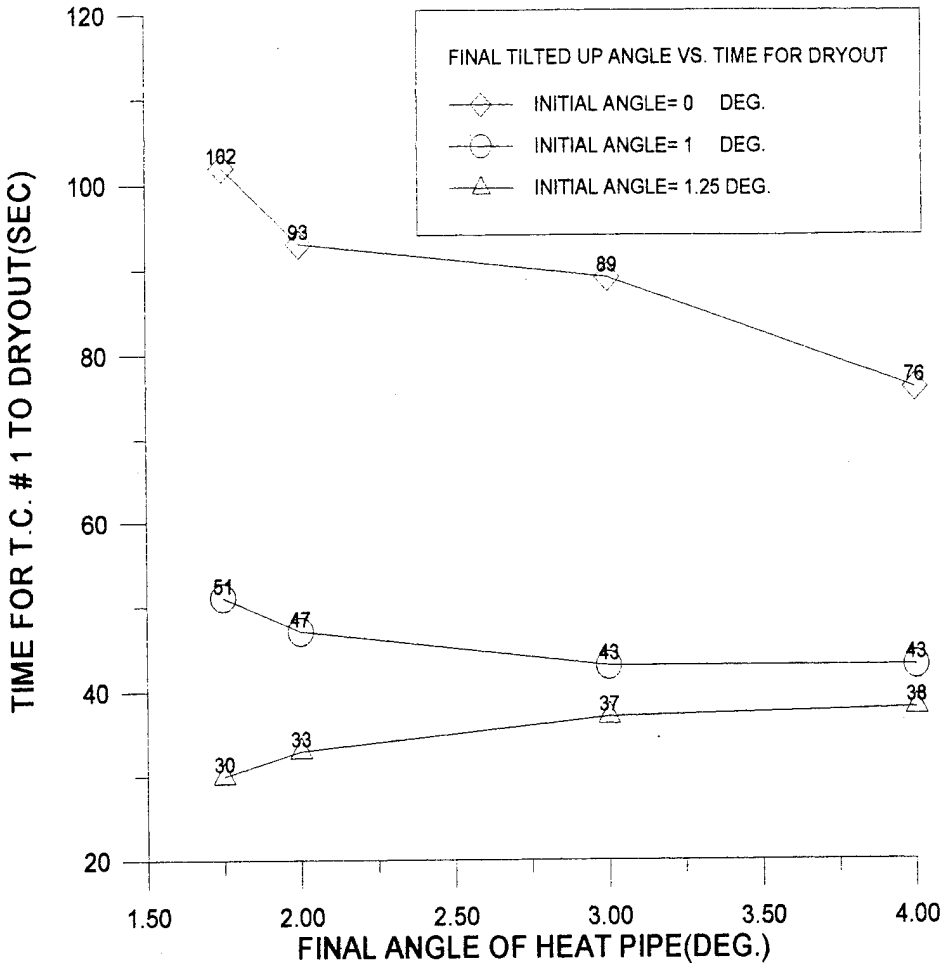

Figure 4.3 Time for TC1 to Dry Out vs. the Final Inclination Angle

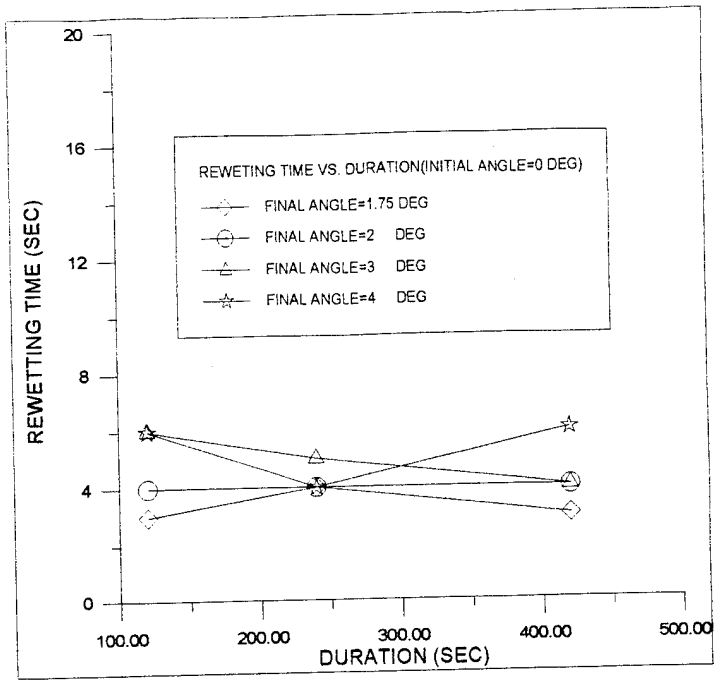

(a)

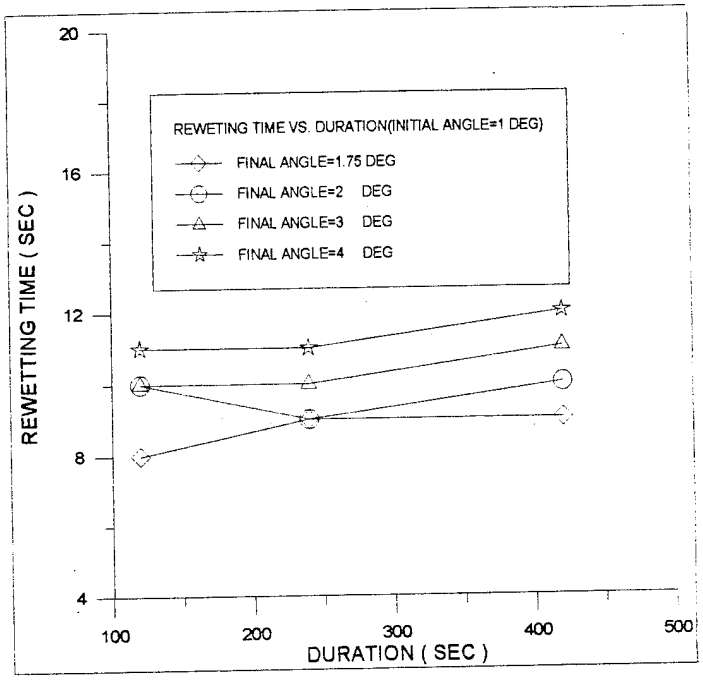

(b)

Figure 4.4(a)(b) Time for TC1 to Rewet vs. Test Duration

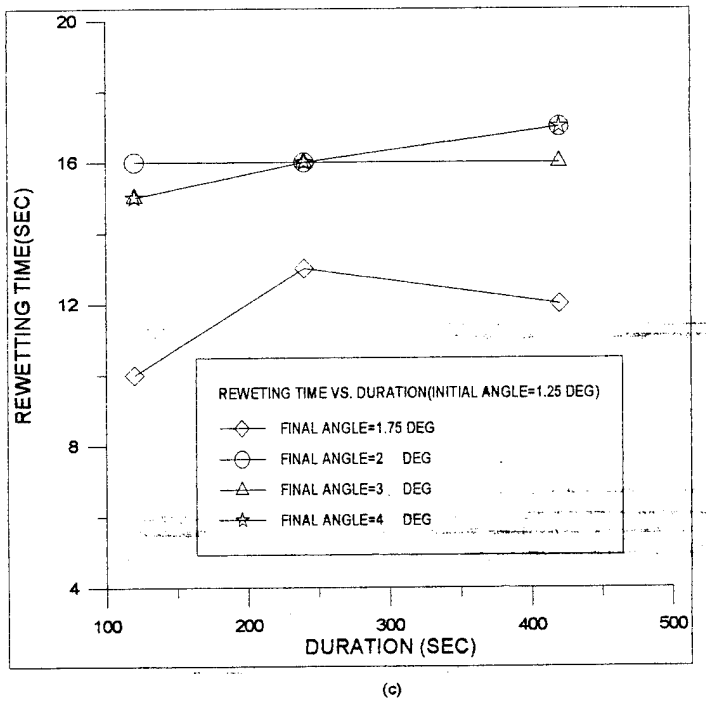

Figure 4.4(c) Time for TC1 to Rewet vs. Test Duration

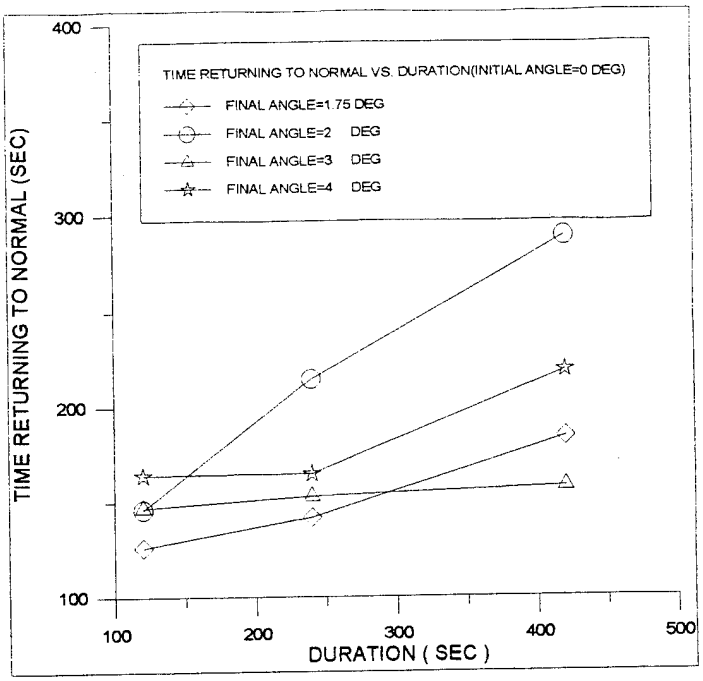

(a)

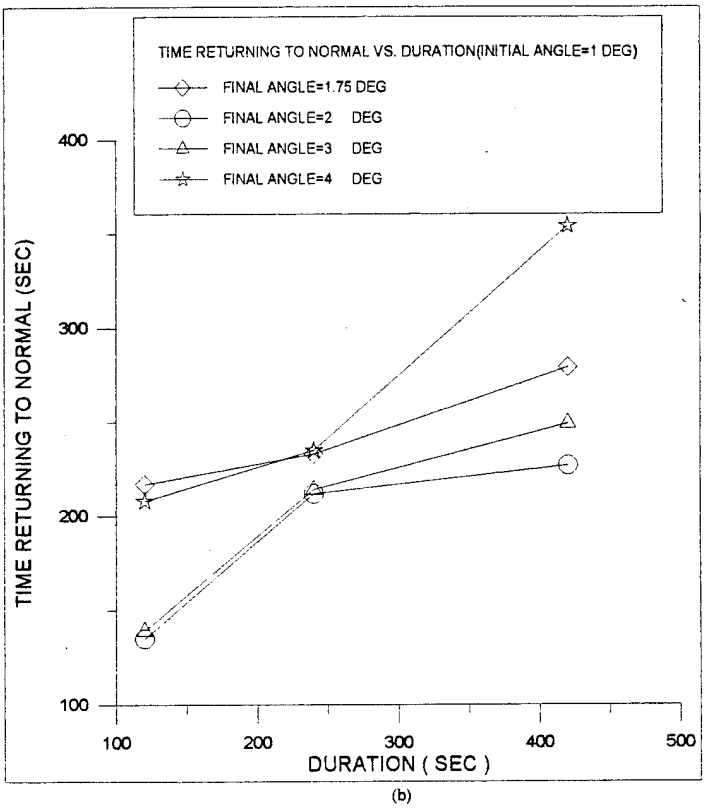

(b)

Figure 4.5(a)(b) Time for TC1 to Return to the Initial Condition vs. Test Duration

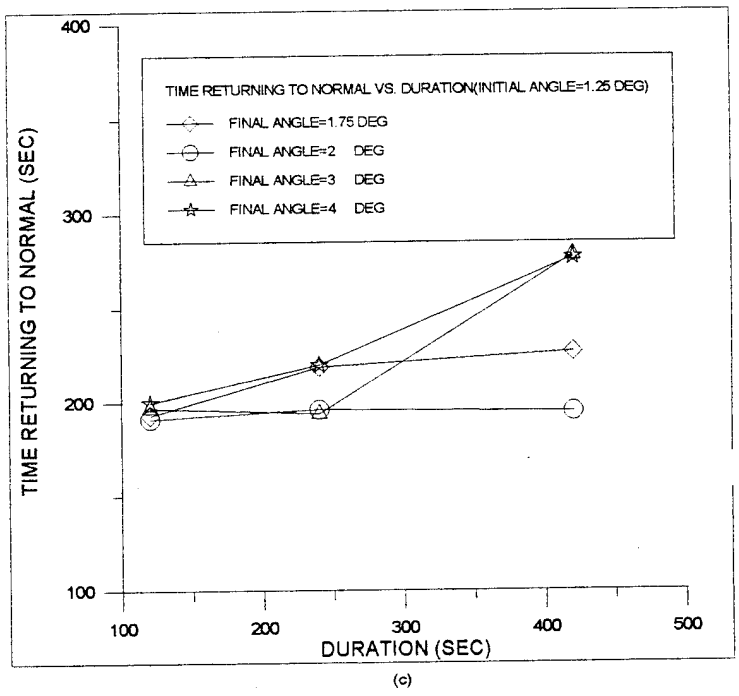

Figure 4.5(c) Time for TC1 to Return to the Initial Condition vs. Test Duration

V. *Conclusions and Recommendations*

This chapter will present a brief review of the entire experiment and succinct conclusions about this research will be made. Several recommendations for follow-on research will be given as well.

5.1 Review for the whole experiment

This study investigated the effect of transient body forces on the performance of an ammonia/axial grooved heat pipe, simulating this heat pipe being used in an accelerating aerospace vehicle.

Under steady state conditions, the heat pipe was tilted to different inclination angles and was held there for a period of time until dried out was observed. The experimental dryout length results were compared with theory.

Under transient conditions, the heat pipe was tilted from different initial inclination angles to different final inclination angles. The time for the heat pipe to dry out, rewet, and return to the initial condition were observed as a function of initial inclination angles, final inclination angles,and duration of heat pipe at the final inclination angle.

5.2 Conclusions

From the results of the experiment mentioned above, the conclusions of this research were summarized as follows:

1. Under steady state conditions, the percent error between the experimental and theoretical data differed by as low as 50 %.
2. Under steady state conditions, body forces influenced the liquid in a heat pipe wick. The larger the body force (or the larger the inclination angle), the larger the dryout length.

3. Under transient conditions, the higher the final angle, the longer the time required for the groove wick heat pipe to rewet after dryout caused by inclination.

4. Under transient conditions, the initial angle had a strong effect on the rewetting time. The higher the initial angle, the longer the rewetting time. The duration of the adverse angle had less of an effect on the time to rewet.

5. Under transient conditions, the groove wick heat pipe took longer time to return to its initial condition after experiencing increased inclination angle and larger duration at the increased angle

5.3 Recommendations

There are some areas left for improving this investigation and some possibilities for follow-on work:

1. Consider another heat source, so as to get higher heat transfer into the heat pipe.

2. Improve the Data Acquisition System (DAS). Since the collected signals of temperatures from all TCs fluctuated quite a lot, a better device was needed to be used to screen them.

3. Improve the insulation condition. Since there was some heat intrusion from the environment through connecters on the flow meter, etc., better insulation needs to be considered when the whole system is set up.

4. Vary the coolant bath temperatures to observe its effect on the experimental results.

Appendix A. Experimental Equipment

Other than the heat pipe itself, the equipment for this experiment consisted of three major subsystems. They were the Coolant System, the Data Acquisition System, and the Support System. The equipment arrangement is shown in Fig. A.1.

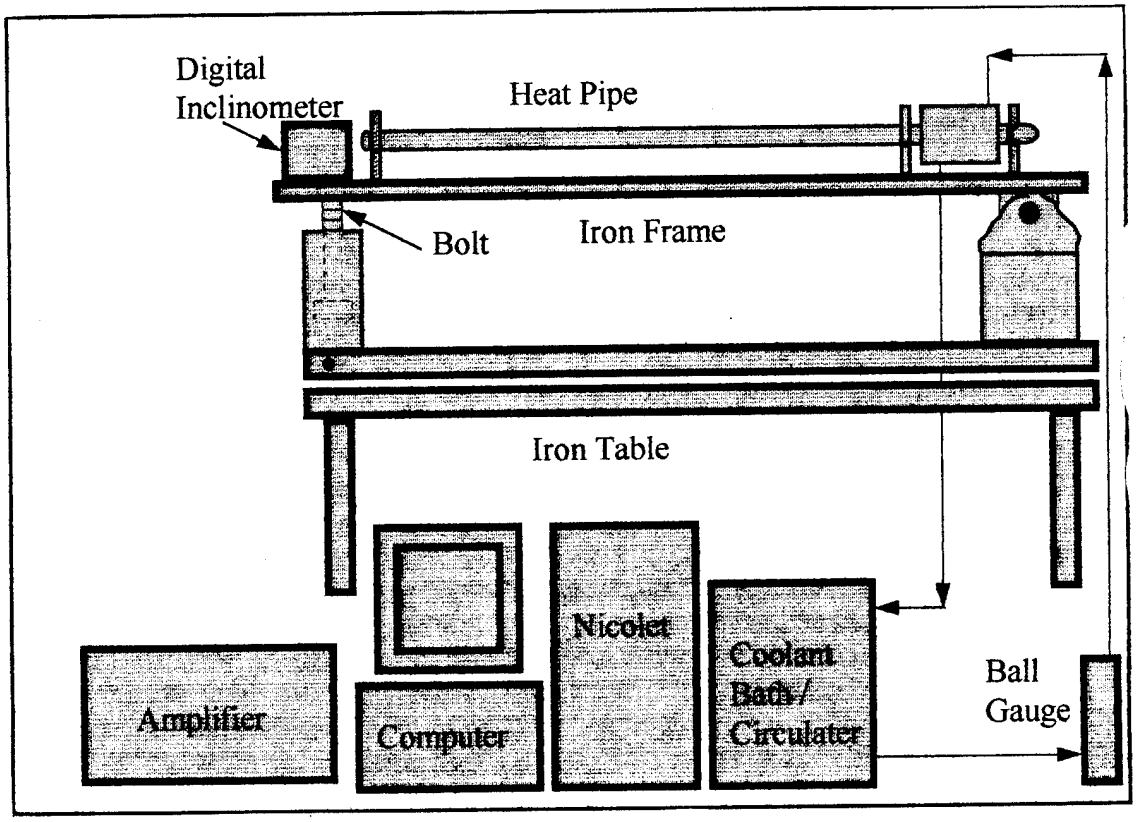

Figure A.1 The Arrangement of the Experimental Equipment

A.1 Coolant System

The coolant system was used as the heat sink to maintain the temperature of the condenser end of the heat pipe. In addition, by adjusting the coolant temperature and flow rate, the operating temperature of the heat pipe was controlled. The main component of the coolant system was the NESLAB RTE-100 Refrigerated Bath/Circulator. This device maintained the coolant fluid at a constant temperature, with an accuracy of $\pm$ 0.1 degree C, and provided the coolant flow. The actual flow of the coolant was controlled by a needle valve on a flow gauge. This flow meter had a range from 0 to 150 ml/min. The coolant fluid interacted with the condenser end of the heat pipe inside the coolant manifold. This manifold was constructed of 25.4 mm ID copper tubing, to which copper endplates and 6.35 mm ID inlet and outlet tubes were attached. Tygon tubing was used as the coolant piping. To prevent heat intrusion from the environment, the coolant manifold and the entire coolant loop were insulated with 9.52 millimeters of poly styrene foam insulation to isolate the coolant lines from the outside temperature.

A.2 Data Acquisition System

The data acquisition system was used to display and record pertinent experimental data during each experimental run. The collected data included the heat pipe surface temperatures and coolant water inlet/outlet temperatures. All temperatures were taken using K-type chromel-alumel thermocouples (TCs). All TCs were manufactured by Omega Corporation and had an operating range of -200 to 1250 degree C with an error rating of $\pm$ 2.2 degree C (the range of the error was cited from a document provided by Omega Corporation and the error was minimized to $\pm$ 0.5 degree after doing the calibration for the DAS). For the heat pipe surface temperature measurements, these TCs were attached on the outside of the heat pipe with OB-101 Epoxy Adhesive which was also a product of Omega Corporation. For the coolant fluid inlet and outlet temperature measurements, the TCs were mounted

in the coolant flow loop using T-adapters. The location of the ten TCs used in this experiment were shown in Fig. 3.1.

Since the noise was bigger than the TCs' output signals, an Amplifier was used to enhance the signals before they were acquired by the DAS, and then the signals were cut back to normal when recorded by the 386 PC. These signals were displayed as voltages varying with time when they were collected by the DAS. They were converted from voltages to temperatures for use in later analysis.

A.3 Support System

The final subsystem, the support system, was used to hold the heat pipe and to tilt the heat pipe during the experiment. This system included an iron frame, bolts, and some styrofoam blocks. The iron frame and bolts were manufactured by the Air Force Institute of Technology (AFIT) Model Fabrication Center, and were neatly regulated by Mr. Andy Pitts, Aero/Astro Lab technician. The iron frame was used to hold the heat pipe. The bolts, including both fine and coarse threads, were used to tilt the heat pipe during steady state operating experiments. The styrofoam blocks made in different thickness were used to tilt the heat pipe during transient experiments.

Bibliography

1. Brennan, Patrick J. and Edward J. Kroliczek, "Heat Pipe Design Handbook: Volume II," *NTIS N81-70112.* Towson, Maryland: B & K Engineering, Inc., June 1979.
2. Chi, S. W., *Heat Pipe Theory and Practice: A Source book.*, Washington: Hemisphere Publishing Corporation, 1976
3. Cheng, K. C. and J. P. Zarling. "Applications of Heat Pipes and Thermosyphons in Cold Regions," *Heat Pipe Technology, Volume II: Materials and Applications.*1-32. New York: Begell House Inc. Publishers,1993
4. Dunn, P. and D. A. Reau. *Heat Pipes, 1st Ed.* New York: Pergamon Press, 1976.
5. Richardson, J. W. et. al. "Effect of Longitudinal Vibration on Heat Pipe Performance," *Journal of Astronautical Sciences, 17 n 5:* 259-246 (March-April 1970)
6. Symons, Eugene P. "Wicking of Liquids in Screens," *NASA TN D-7657*, May 1974
7. Shishido, I. and S. Ohtani. "Working Fluid Distribution Within Heat Pipe Wick," *Proceedings of the 5th International Heat Pipe Conference,* Tsukuba, Japan, May 1984
8. Gerasimov, Y. F. et. al. "Performance of Heat Pipe with Separate Vapor and Liquid Ducts Rotating in a Gravity Field," *Heat Transfer-Soviet Research, 17 n 4:* 127-130 (July-August 1985).
9. Kiseev, V. M. et. al. "Influence of Adverse Accelerations on the Operation of an 'Antigravity' Heat Pipe," *Journal of Engineering Physics, 50 n 4:* 394-398 (April 1986)
10. Noda, H. et. al. "A Model for the Heat Transfer Limit of a Screen Wick Heat Pipe," *Heat Transfer-Japanese Research, 18 n 3:* 44-57 (May-June 1989).
11. Hendrix, Walter A. *An Analysis of Body Force Effects on Transient and Steady-State Performance of Heat Pipes.* PhD Dissertation. Georgia Institute of Technology, GA, 1989.
12. Charlton, Capt Mark C. "Effect of Transverse Vibration on the Capillary Limit of a Wrapped Screen Wick Copper/Water Heat Pipe." MS Thesis AFIT/GA/ENY/92D-02. School of Engineering, Air Force Institute of Technology (AU), Wright-Patterson AFB OH, December 1992 (AAJ-4635)

Vita

Major Wen-Lung Wang was born 8 Sept. 1959, in Pintung, Taiwan. He is married to Hui-Yueh Li and has a 7 year-old daughter, Tina, a 3 year-old son, William. He was enrolled in Air Technical College (ATC) in 1978 and received his degree in Mechanical Engineering in 1981. Then, he served 4 years as a maintenance officer at the flight line at the Air Force Base. In 1985, The Chinese Air Force sponsored his undergraduate program at National Chen Kung University in Tainan, where he received his Bachelor Degree in Engineering Science in 1988. He was assigned to Air Technical College as an instructor for 6 years. In 1994, he was selected to enter the Air Force Institute of Technology (AFIT) for his Master of Science Degree in Aeronautical Engineering. Upon graduation, he will still go back to ATC as an instructor.

Permanent address: 108, 235 lane
De tung street
Tainan, Taiwan, R.O.C.

REPORT DOCUMENTATION PAGE

Form Approved
OMB No. 0704-0188

1. AGENCY USE ONLY *(Leave blank)*	2. REPORT DATE	3. REPORT TYPE AND DATES COVERED
	June 1996	Master's Thesis

4. TITLE AND SUBTITLE
Effect of Body Force on the Performance of an Axial Grooved Heat Pipe

5. FUNDING NUMBERS

6. AUTHOR(S)
Wen-Lung, Wang, Maj, CAF

7. PERFORMING ORGANIZATION NAME(S) AND ADDRESS(ES)
Air Force Institute of Technology, WPAFB OH 45433-6583

8. PERFORMING ORGANIZATION REPORT NUMBER

9. SPONSORING/MONITORING AGENCY NAME(S) AND ADDRESS(ES)
Dr. Jerry Beam
Wright Laboratory
Aero Propulsion & Power Directorate
WL/POO

10. SPONSORING/MONITORING AGENCY REPORT NUMBER

11. SUPPLEMENTARY NOTES

12a. DISTRIBUTION/AVAILABILITY STATEMENT
Approved for public release; distribution unlimited

12b. DISTRIBUTION CODE
A

13. ABSTRACT *(Maximum 200 words)*

An experimental investigation was performed to determine the effect of transient body forces on the performance of an ammonia/axial groove heat pipe. The effects of increased body forces on the dryout and rewet performance were simulated by tilting the heat pipe to different inclination angles. Theoretical calculations predicted the dryout length varied with different final inclination angles. The steady state experimental work was performed by tilting the heat pipe from 0 degrees to different final inclination angles for a period of time until total dryout occurred. Then, from the plot of the changing temperature at each location along the heat pipe, the dryout length could be predicted. Under steady state condition, the percent error between the experimental and theoretical data differed by as low as 50 %. The transient experimental work was performed by tilting the heat pipe from different initial inclination angles to different final inclination angles under three duration conditions. The time for the heat pipe to dryout, rewet, and return to the initial condition was observed as a function of the initial inclination angles, the final inclination angles, and duration of the heat pipe at the final angle. The results revealed that the larger body force increased the dryout length, and increased the time to return to its initial condition.

14. SUBJECT TERMS
Heat Pipe, Body Force, Axial Groove

15. NUMBER OF PAGES
60

16. PRICE CODE

17. SECURITY CLASSIFICATION OF REPORT	18. SECURITY CLASSIFICATION OF THIS PAGE	19. SECURITY CLASSIFICATION OF ABSTRACT	20. LIMITATION OF ABSTRACT
Unclassified	Unclassified	Unclassified	UL

GENERAL INSTRUCTIONS FOR COMPLETING SF 298

The Report Documentation Page (RDP) is used in announcing and cataloging reports. It is important that this information be consistent with the rest of the report, particularly the cover and title page. Instructions for filling in each block of the form follow. It is important to ***stay within the lines*** to meet ***optical scanning requirements***.

Block 1. Agency Use Only *(Leave blank)*.

Block 2. Report Date. Full publication date including day, month, and year, if available (e.g. 1 Jan 88). Must cite at least the year.

Block 3. Type of Report and Dates Covered. State whether report is interim, final, etc. If applicable, enter inclusive report dates (e.g. 10 Jun 87 - 30 Jun 88).

Block 4. Title and Subtitle. A title is taken from the part of the report that provides the most meaningful and complete information. When a report is prepared in more than one volume, repeat the primary title, add volume number, and include subtitle for the specific volume. On classified documents enter the title classification in parentheses.

Block 5. Funding Numbers. To include contract and grant numbers; may include program element number(s), project number(s), task number(s), and work unit number(s). Use the following labels:

C	- Contract	**PR**	- Project
G	- Grant	**TA**	- Task
PE	- Program Element	**WU**	- Work Unit Accession No.

Block 6. Author(s). Name(s) of person(s) responsible for writing the report, performing the research, or credited with the content of the report. If editor or compiler, this should follow the name(s).

Block 7. Performing Organization Name(s) and Address(es). Self-explanatory.

Block 8. Performing Organization Report Number. Enter the unique alphanumeric report number(s) assigned by the organization performing the report.

Block 9. Sponsoring/Monitoring Agency Name(s) and Address(es). Self-explanatory.

Block 10. Sponsoring/Monitoring Agency Report Number. *(If known)*

Block 11. Supplementary Notes. Enter information not included elsewhere such as: Prepared in cooperation with...; Trans. of...; To be published in.... When a report is revised, include a statement whether the new report supersedes or supplements the older report.

Block 12a. Distribution/Availability Statement. Denotes public availability or limitations. Cite any availability to the public. Enter additional limitations or special markings in all capitals (e.g. NOFORN, REL, ITAR).

- **DOD** - See DoDD 5230.24, "Distribution Statements on Technical Documents."
- **DOE** - See authorities.
- **NASA** - See Handbook NHB 2200.2.
- **NTIS** - Leave blank.

Block 12b. Distribution Code.

- **DOD** - Leave blank.
- **DOE** - Enter DOE distribution categories from the Standard Distribution for Unclassified Scientific and Technical Reports.
- **NASA** - Leave blank.
- **NTIS** - Leave blank.

Block 13. Abstract. Include a brief *(Maximum 200 words)* factual summary of the most significant information contained in the report.

Block 14. Subject Terms. Keywords or phrases identifying major subjects in the report.

Block 15. Number of Pages. Enter the total number of pages.

Block 16. Price Code. Enter appropriate price code *(NTIS only)*.

Blocks 17. - 19. Security Classifications. Self-explanatory. Enter U.S. Security Classification in accordance with U.S. Security Regulations (i.e., UNCLASSIFIED). If form contains classified information, stamp classification on the top and bottom of the page.

Block 20. Limitation of Abstract. This block must be completed to assign a limitation to the abstract. Enter either UL (unlimited) or SAR (same as report). An entry in this block is necessary if the abstract is to be limited. If blank, the abstract is assumed to be unlimited.